Modern Accelerator-Based Neutrino Detectors

Brooke Russell (MIT)

17th International Neutrino Summer School @ UC Santa Barbara

June 30, 2026

Revisiting The Plan

Lecture 1 (yesterday)

- Motivate neutrino detection inference through *detector response*
  - ➔ Establish the framework for important aspects of detector design

Lecture 2 (today)

- Neutrino flux specific *full response* (detector response ⊗ electronics response) optimization
  - ➔Modern accelerator-based neutrino experiment case studies in instrument application

Content shown here is germane to >100 MeV neutrino detection

➔ See P. Barbeau for <100 MeV neutrino detection

Detected Neutrino Detectors at the LHC

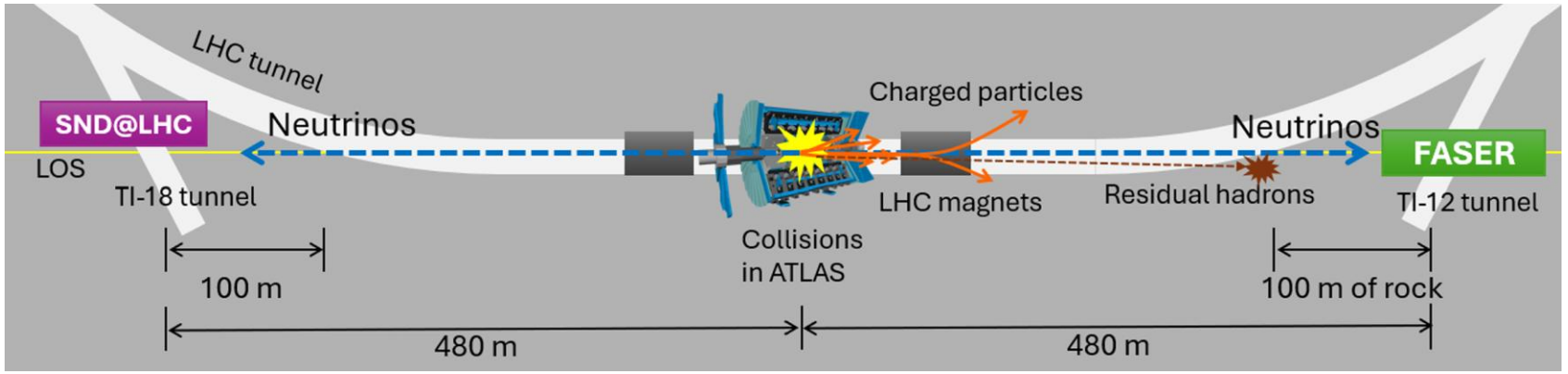

A. Ariga, J. Boyd, F. Kling, A. De Roeck, *Annu. Rev. Nucl. Part. Sci.* 2025. 75:57-81

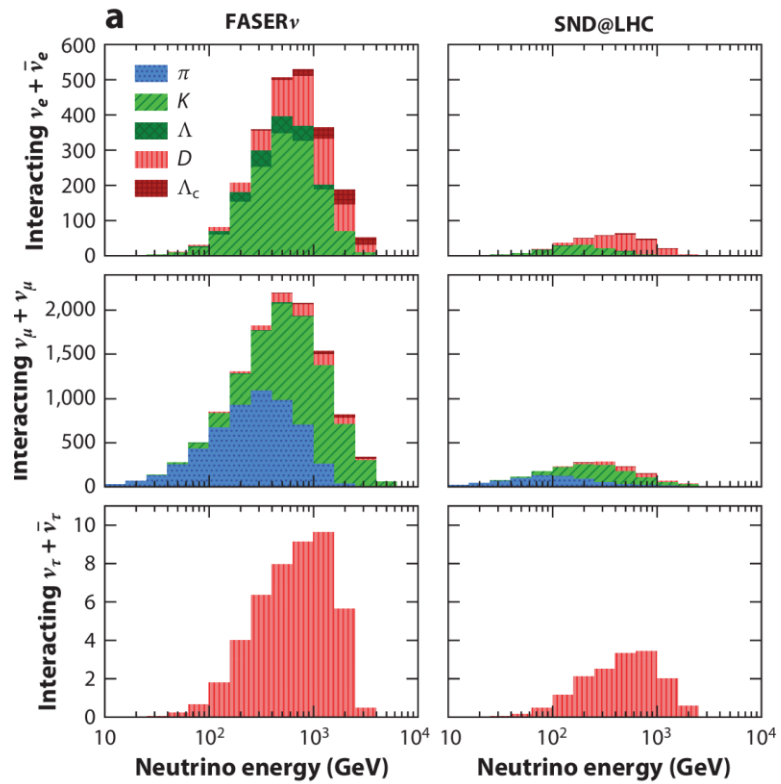

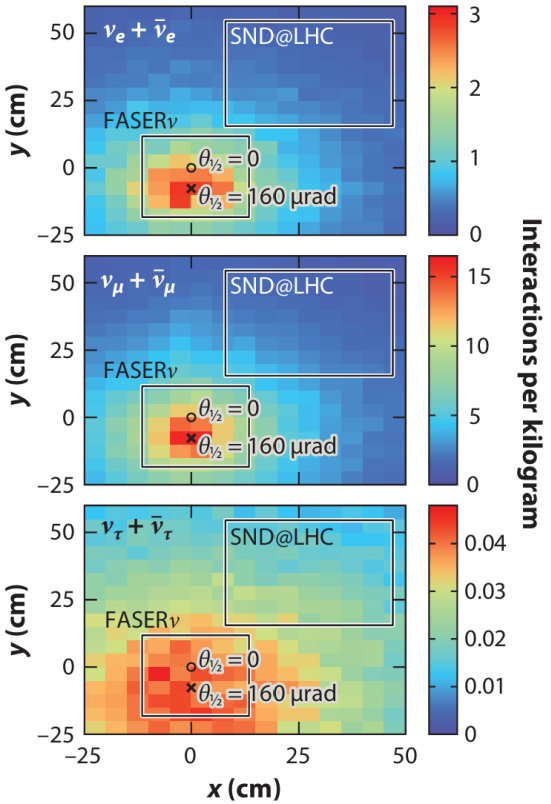

FASER
(Forward Search Experiment)

1,100 kg tungsten target composed of 730 plates interleaved with nuclear emulsion films

- 220 radiation lengths
- 7.8 hadronic interaction lengths

$\eta > 8.8$ pseudorapidity coverage

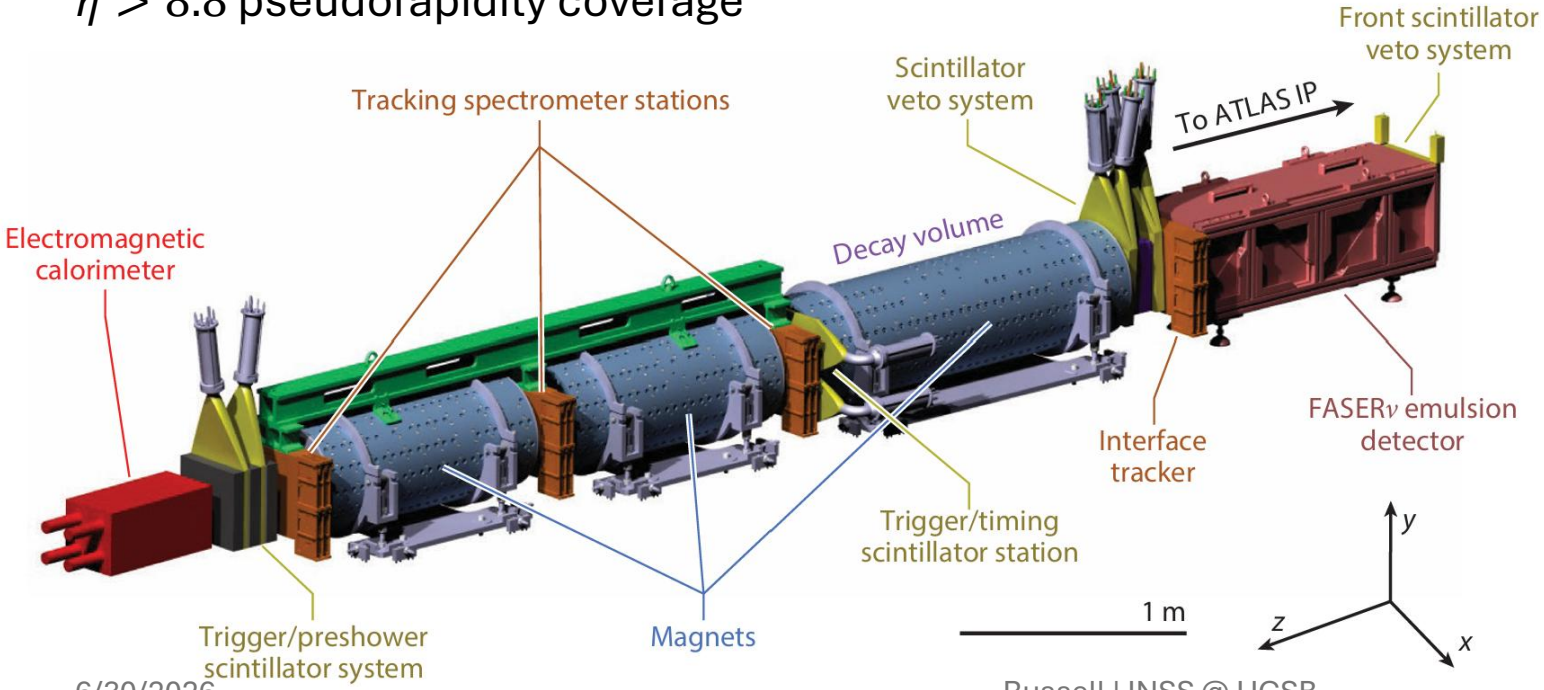

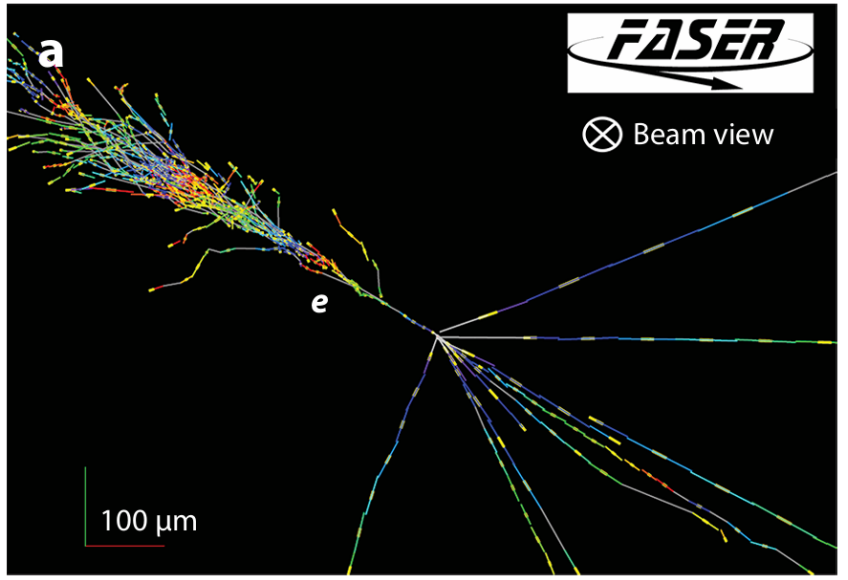

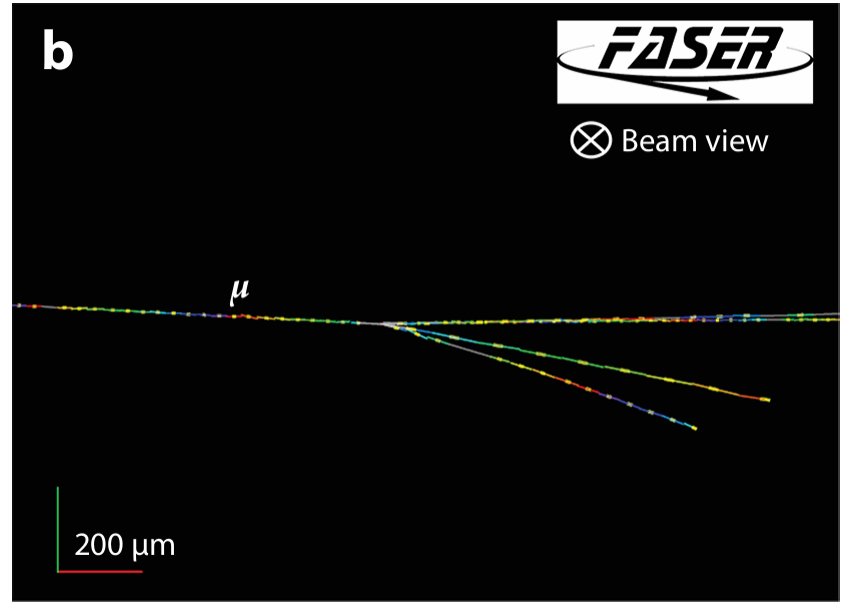

SND@LHC
(Scattering and Neutrino Detector at the Large Hadron Collider)

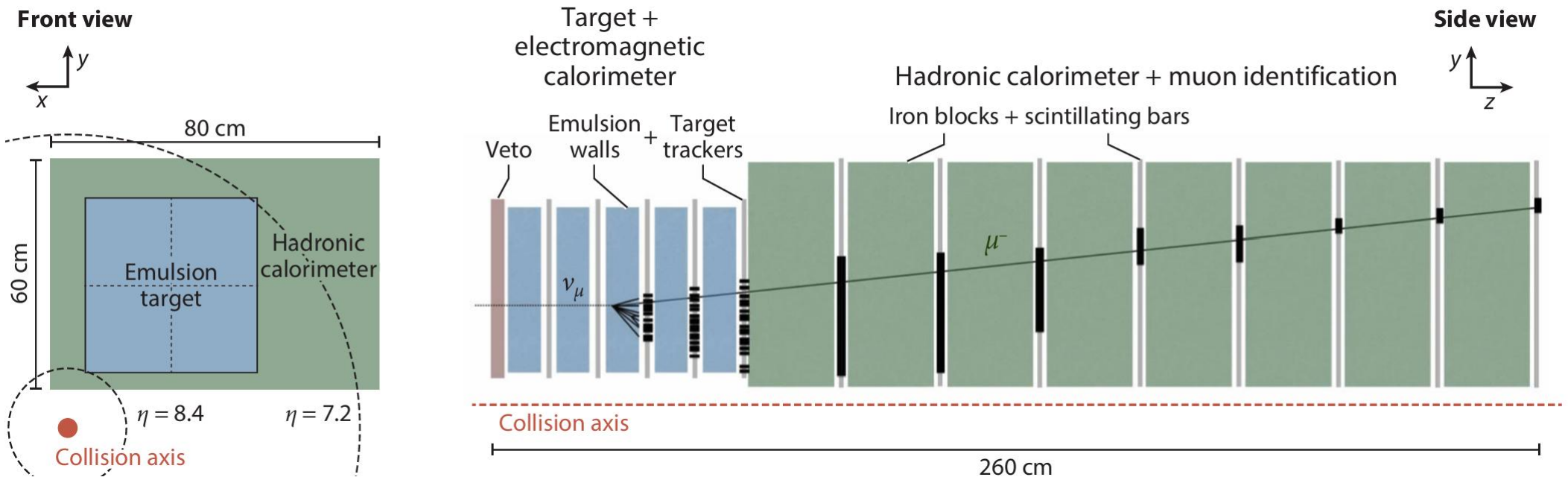

Neutrino Energy Reconstruction

➔ See L. Fields on neutrino flux determination
➔ See T. Katori on neutrino interactions
➔ See Z. Vallari on long baseline experiments

Kinematic method

T2K
HyperK

$$E_\nu^{QE,rec} = \frac{m_p^2 - m_l^2 - (m_n - E_b)^2 + 2E_l(m_n - E_b)}{2(m_n - E_b - E_l + p_l^z)}$$

Calorimetric method

NOvA
DUNE

$$E_\nu^{rec,\,avail} = E_l + E_{had}^{avail} = E_l + \sum_{i=p} T_i + \sum_{i=\pi^\pm,\pi^0,\gamma,h} E_i$$

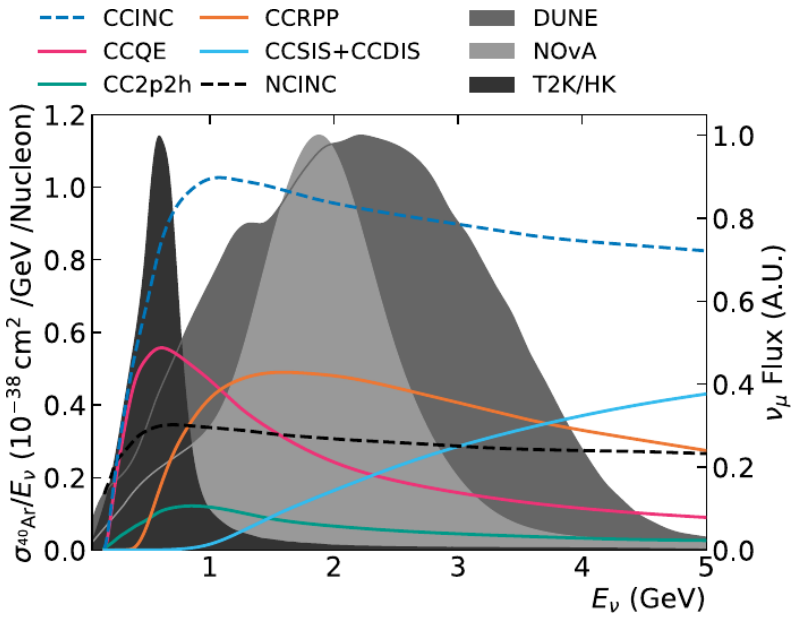

Channel		Hyper-K/T2K	NOvA	DUNE
ν_μ	CCQE	42.0%	17.2%	19.6%
	CC2p2h	8.3%	4.6%	5.3%
	CCRPP	35.1%	41.6%	40.1%
	CCSIS/DIS	13.5%	34.7%	33.3%
$\bar{\nu}_\mu$	CCQE	54.6%	31.3%	23.9%
	CC2p2h	11.2%	7.1%	8.6%
	CCRPP	25.9%	38.5%	44.5%
	CCSIS/DIS	6.2%	20.0%	21.1%

Neutrino Energy Reconstruction

➔ See L. Fields on neutrino flux determination
➔ See T. Katori on neutrino interactions
➔ See Z. Vallari on long baseline experiments

Kinematic method

T2K
HyperK

$$E_\nu^{QE,rec} = \frac{m_p^2 - m_l^2 - (m_n - E_b)^2 + 2E_l(m_n - E_b)}{2(m_n - E_b - E_l + p_l^z)}$$

Calorimetric method

NOvA
DUNE

$$E_\nu^{rec,\,avail} = E_l + E_{had}^{avail} = E_l + \sum_{i=p} T_i + \sum_{i=\pi^\pm,\pi^0,\gamma,h} E_i$$

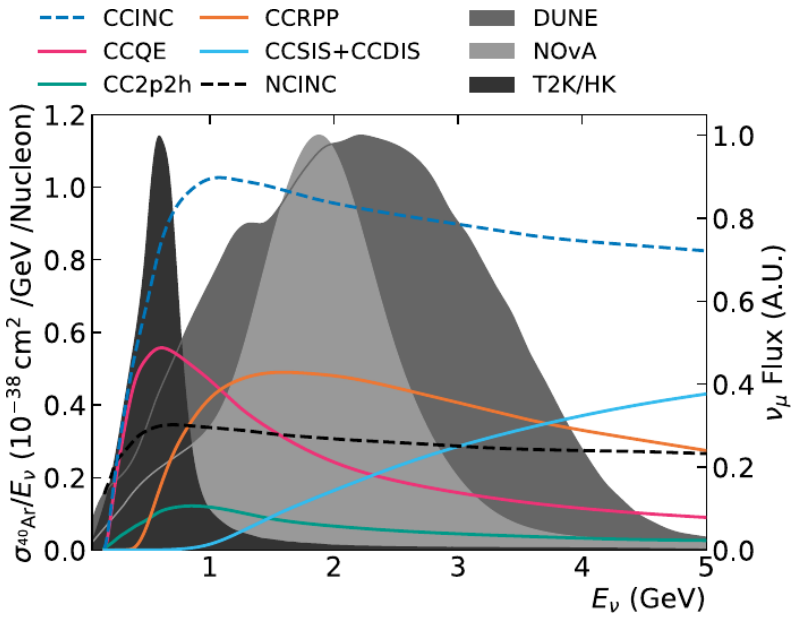

Channel		Hyper-K/T2K	NOvA	DUNE
ν_μ	CCQE	42.0%	17.2%	19.6%
	CC2p2h	8.3%	4.6%	5.3%
	CCRPP	35.1%	41.6%	40.1%
	CCSIS/DIS	13.5%	34.7%	33.3%
$\bar{\nu}_\mu$	CCQE	54.6%	31.3%	23.9%
	CC2p2h	11.2%	7.1%	8.6%
	CCRPP	25.9%	38.5%	44.5%
	CCSIS/DIS	6.2%	20.0%	21.1%

Cherenkov Effect

If speed of charged particle exceeds speed of light in a dielectric medium of index of refraction n, a "shock wave" of radiation develops at a critical angle $cos\theta_C = \frac{1}{\beta n}$ where $\beta > \frac{1}{n}$

Particle detection momentum threshold:

$$p_{thresh} = m\sqrt{\frac{1}{n^2-1}}$$

For water (n=1.3)

- 0.6 MeV electron threshold
- 120 MeV muon threshold
- 160 MeV pion threshold
- 1.1 GeV proton threshold

- Operating principle of Cherenkov detectors

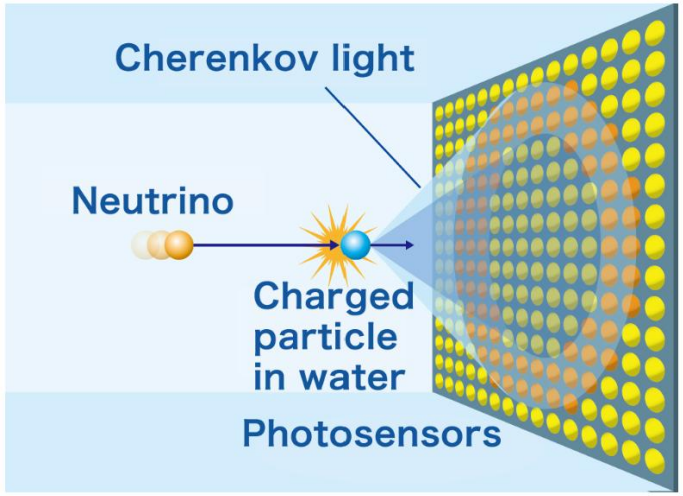

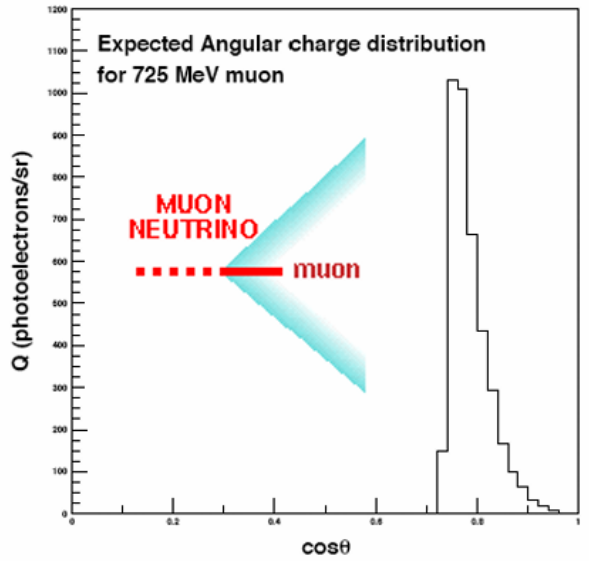

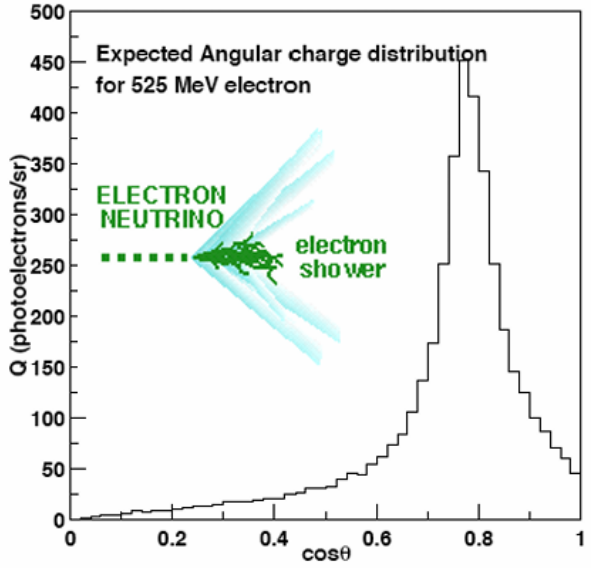

Figures from M. Earl's PhD Thesis

T2K

- Neutrino energy reconstruction from lepton kinematics

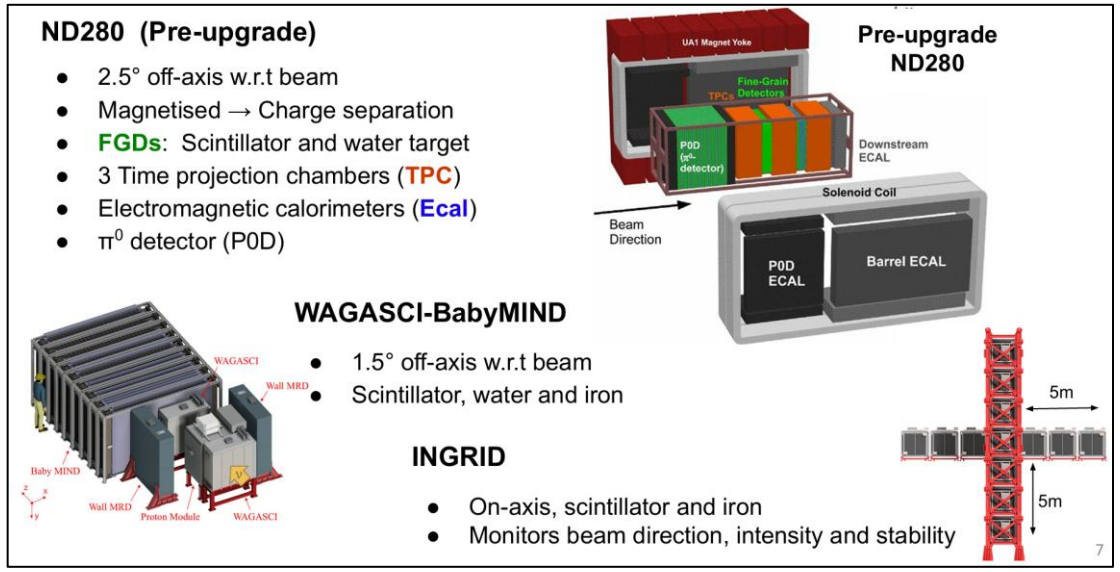

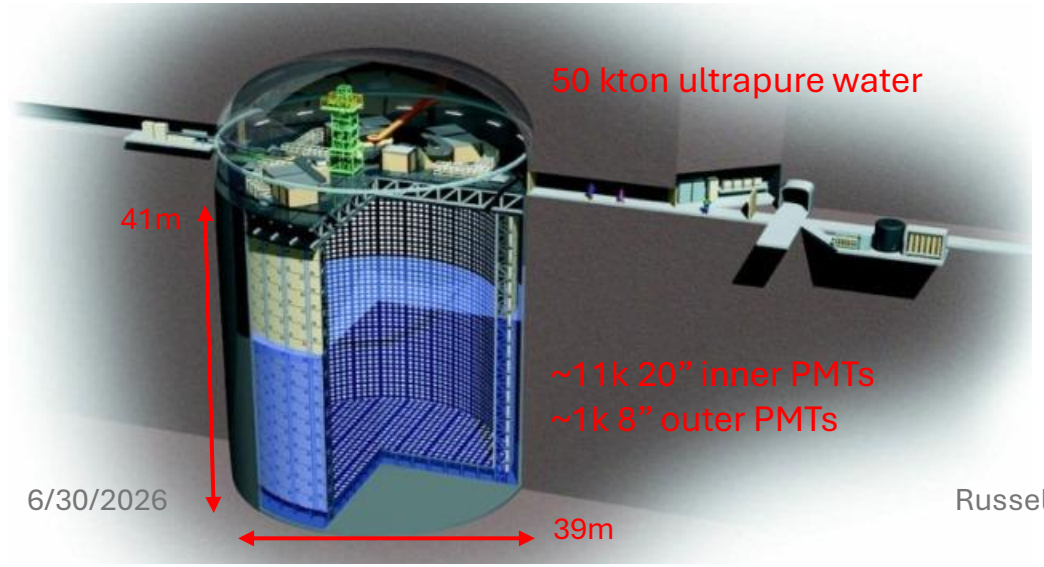

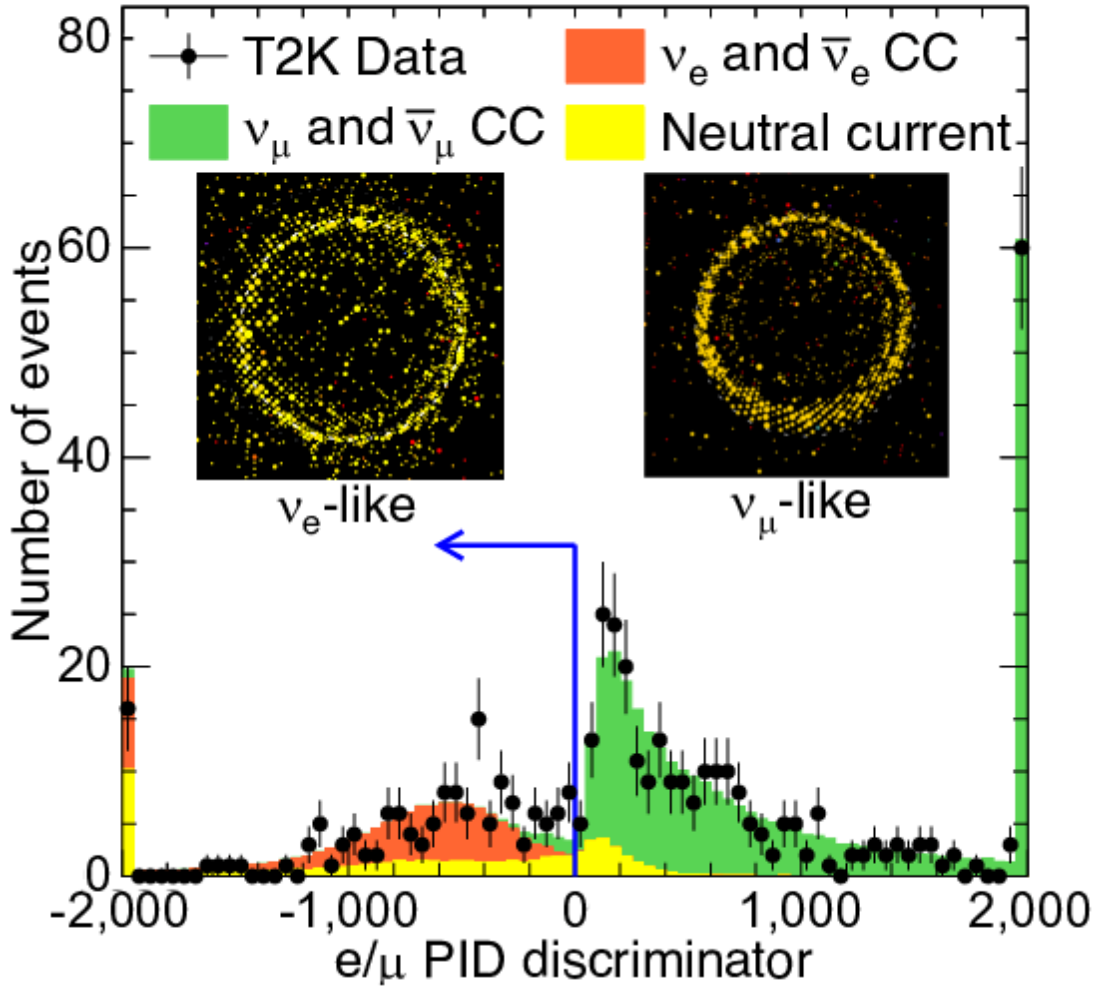

- Neutrino energy reconstruction from lepton kinematics

HyperKamiokande

~40% photocoverage!

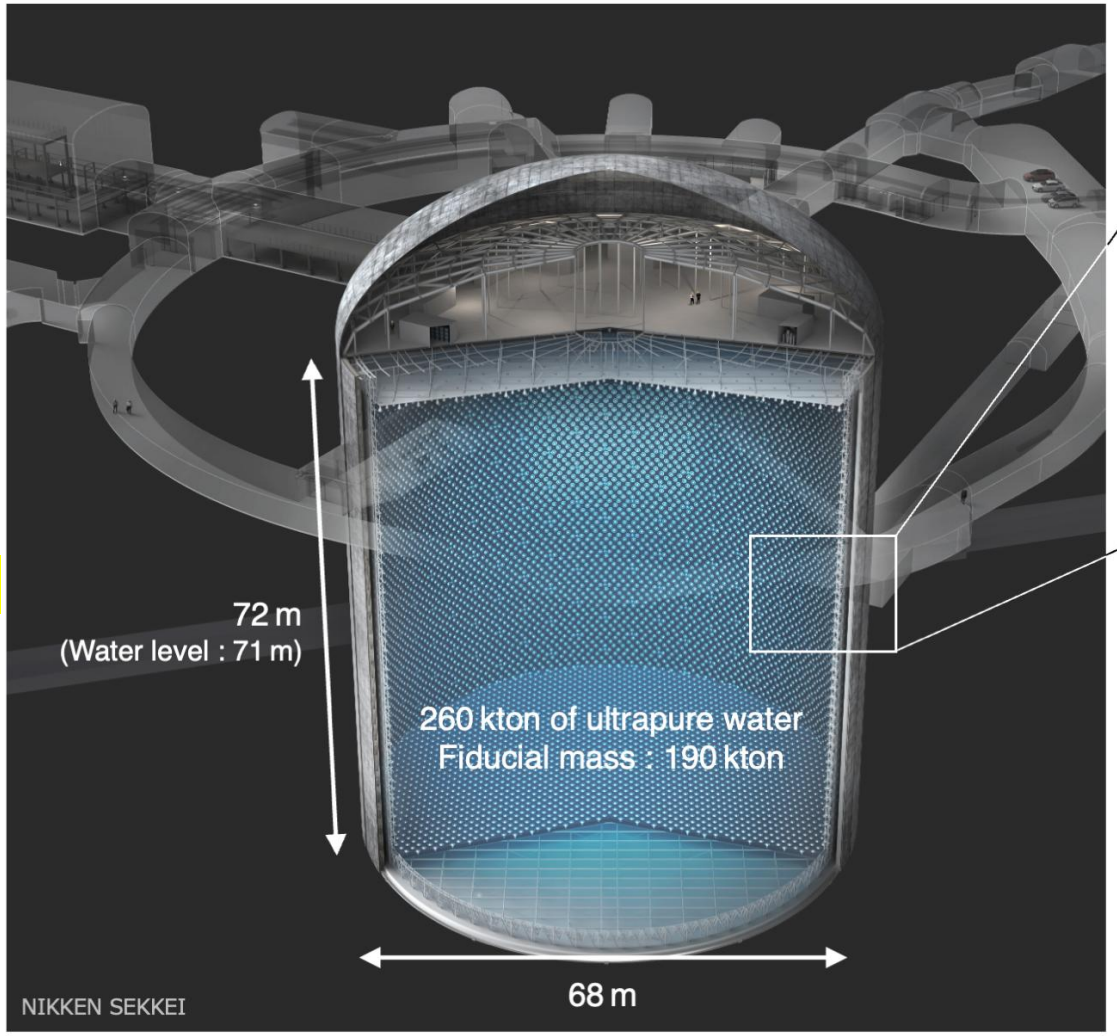

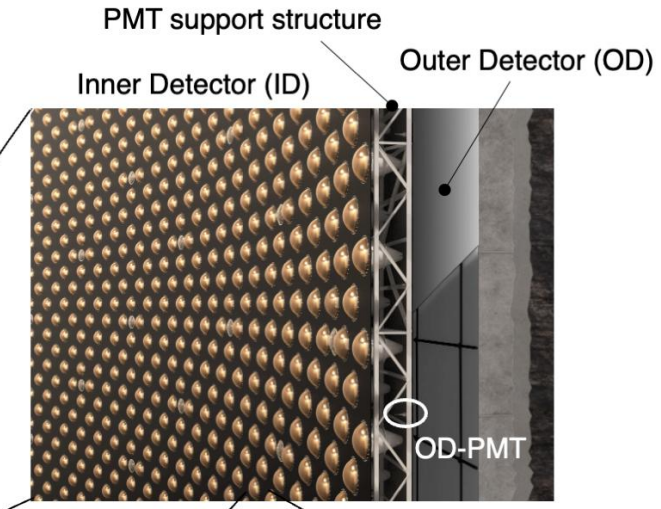

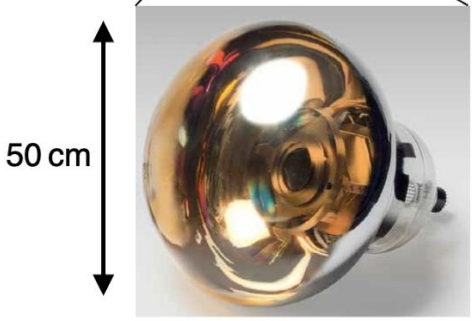

©Hamamatsu Photonics K.K.
New ultrasensitive ID-PMT

Near Detectors

R. Akutsu Neutrino2026

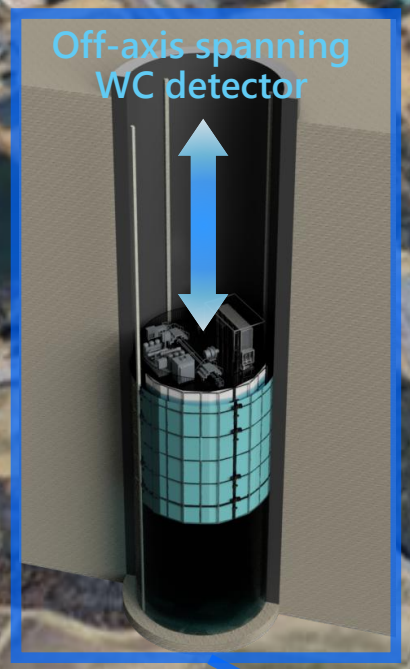

IWCD
(Intermediate Water Cherenkov Detector)

ν production target

280m

870m

Hyper-K

ND280

Upgraded in 2024, followed by successful data taking
→ ***T2K talk*** by Sophie King

Future upgrade ideas;

- "*ND280++, the multi-ton upgrade of the magnetised near detector for the Hyper-Kamiokande high-statistics phase*" by **Daniel Ferlewicz**
- "*Development and Performance Evaluation of a Tracking Detector Using Water-based Liquid Scintillator for the Hyper-Kamiokande Experiment*" by **Koki Hayashi**

IWCD Detector

R. Akutsu Neutrino2026

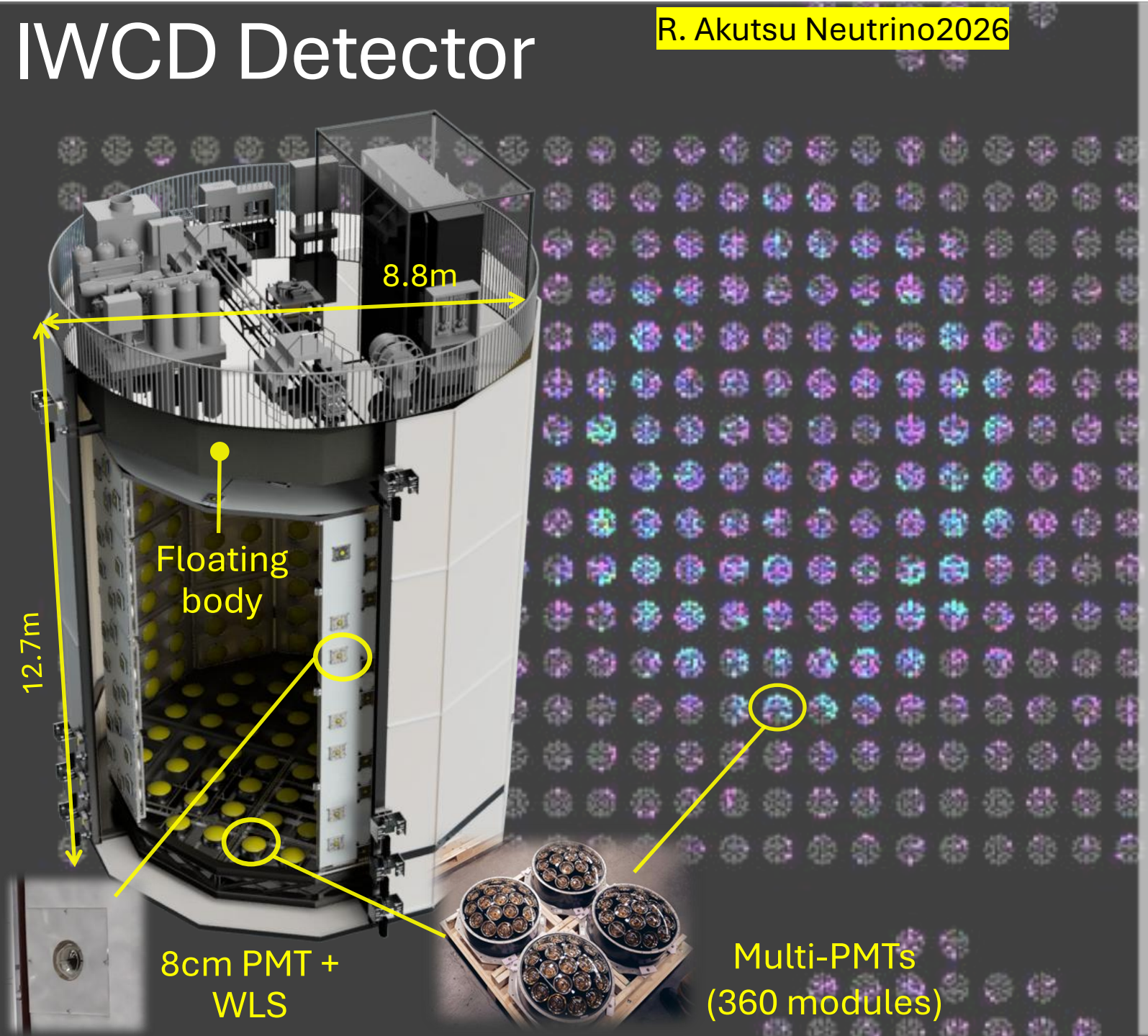

- Vertically movable water Cherenkov detector, covering off-axis angle of 1.5 – 4 degrees

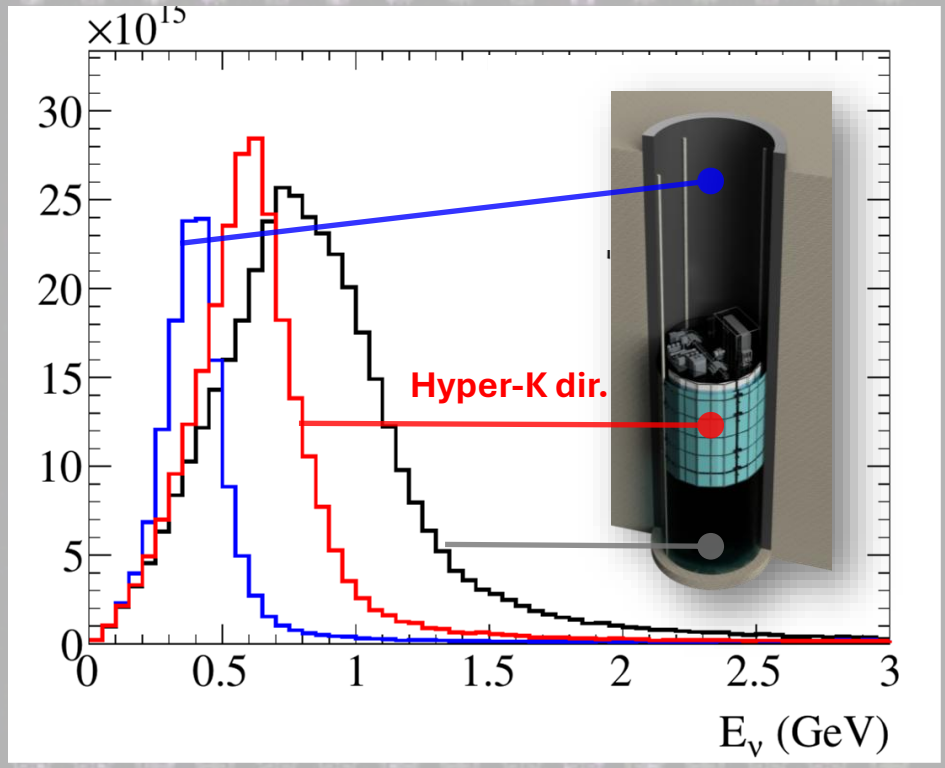

- ~110t fiducial mass to be used for $\nu_e/\bar{\nu}_e$ measurements
  - >10k signal events for each in 10 years

Neutrino Energy Reconstruction

➔ See L. Fields on neutrino flux determination
➔ See T. Katori on neutrino interactions
➔ See Z. Vallari on long baseline experiments

Kinematic method

T2K
HyperK

$$E_\nu^{QE,rec} = \frac{m_p^2 - m_l^2 - (m_n - E_b)^2 + 2E_l(m_n - E_b)}{2(m_n - E_b - E_l + p_l^z)}$$

Calorimetric method

NOvA
DUNE

$$E_\nu^{rec,\,avail} = E_l + E_{had}^{avail} = E_l + \sum_{i=p} T_i + \sum_{i=\pi^\pm,\pi^0,\gamma,h} E_i$$

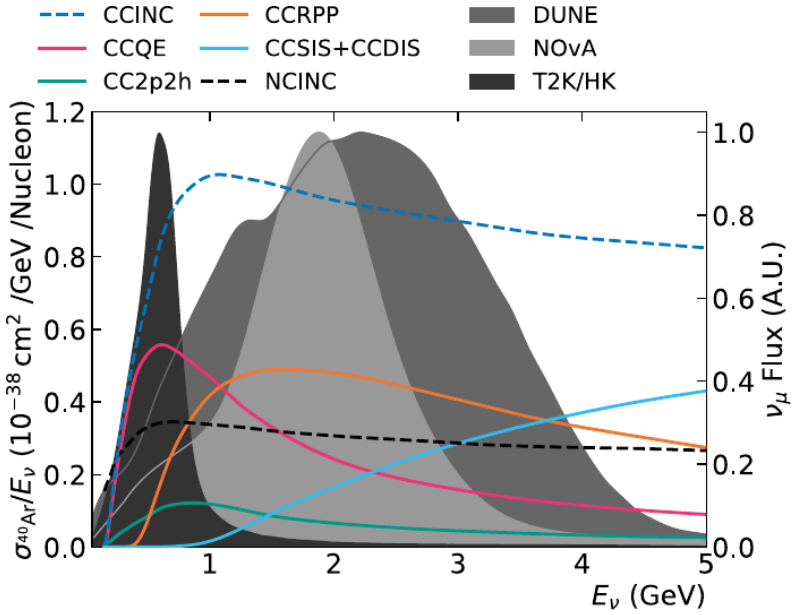

Channel		Hyper-K/T2K	NOvA	DUNE
ν_μ	CCQE	42.0%	17.2%	19.6%
	CC2p2h	8.3%	4.6%	5.3%
	CCRPP	35.1%	41.6%	40.1%
	CCSIS/DIS	13.5%	34.7%	33.3%
$\bar{\nu}_\mu$	CCQE	54.6%	31.3%	23.9%
	CC2p2h	11.2%	7.1%	8.6%
	CCRPP	25.9%	38.5%	44.5%
	CCSIS/DIS	6.2%	20.0%	21.1%

NOvA

Functionally identical segmented liquid scintillator detector

- ND: ~290 t and ~100 m underground
- FD: ~14 kt and on Earth's surface

➢ Muon energy reconstructed by track length

➢ Calorimetric energy estimation performed separately for EM and hadronic clusters

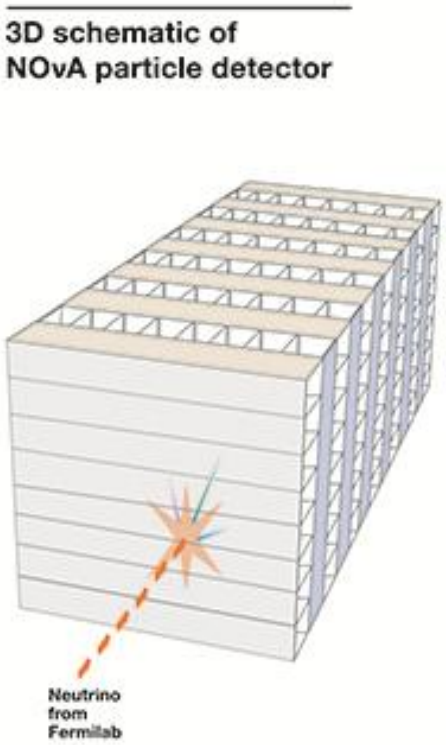

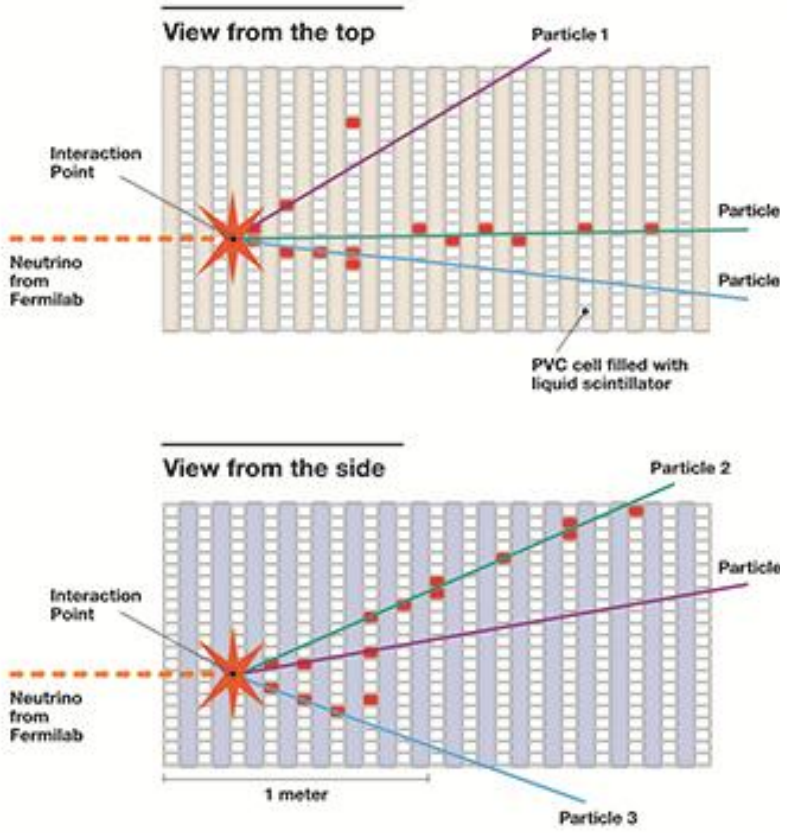

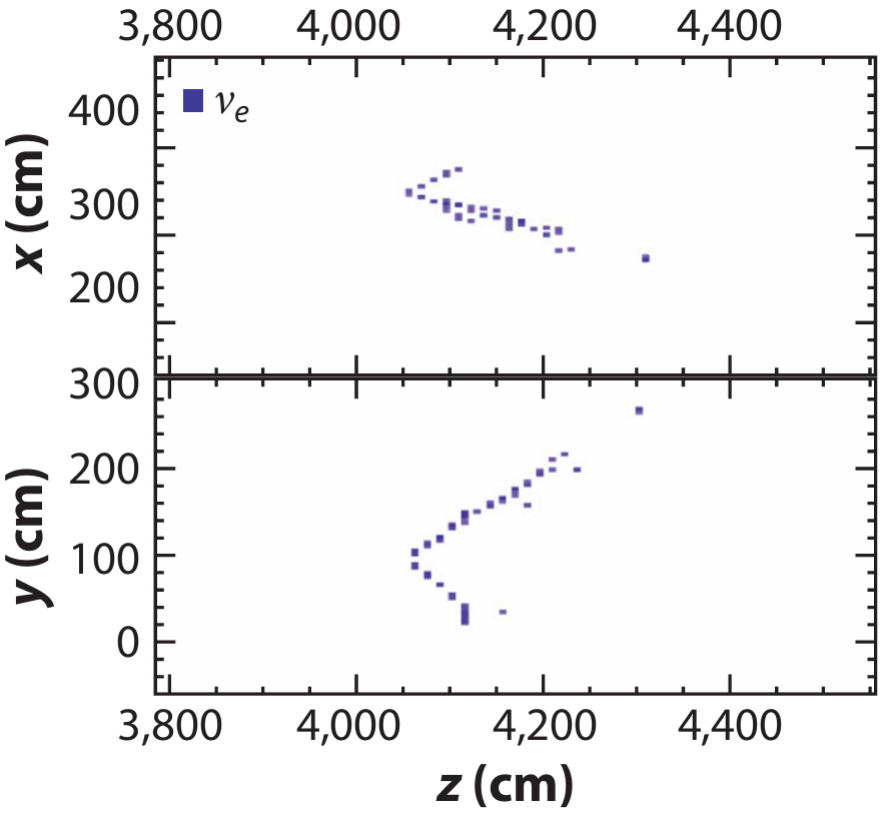

Liquid Argon Time Projection Chamber

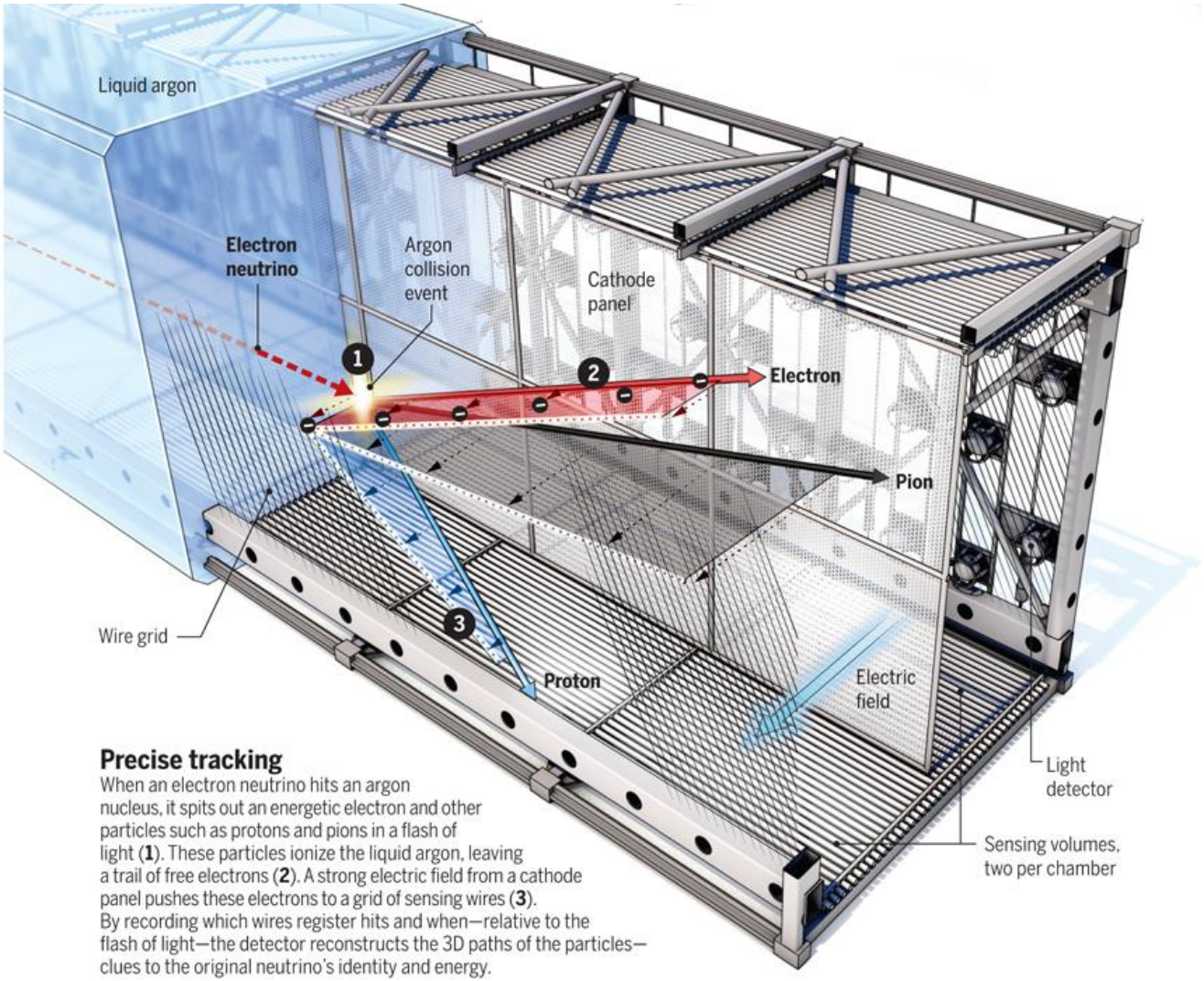

Precise tracking
When an electron neutrino hits an argon nucleus, it spits out an energetic electron and other particles such as protons and pions in a flash of light (**1**). These particles ionize the liquid argon, leaving a trail of free electrons (**2**). A strong electric field from a cathode panel pushes these electrons to a grid of sensing wires (**3**). By recording which wires register hits and when—relative to the flash of light—the detector reconstructs the 3D paths of the particles—clues to the original neutrino's identity and energy.

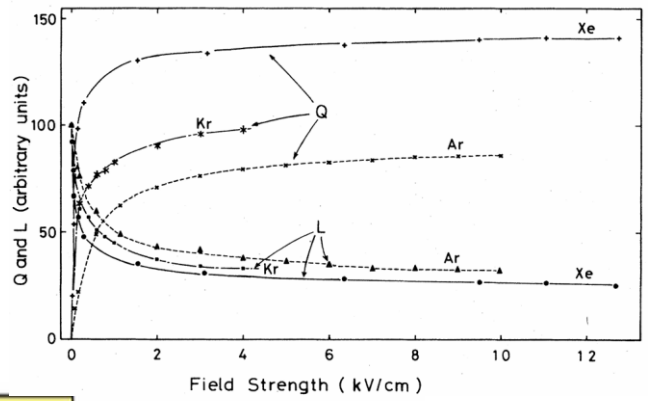

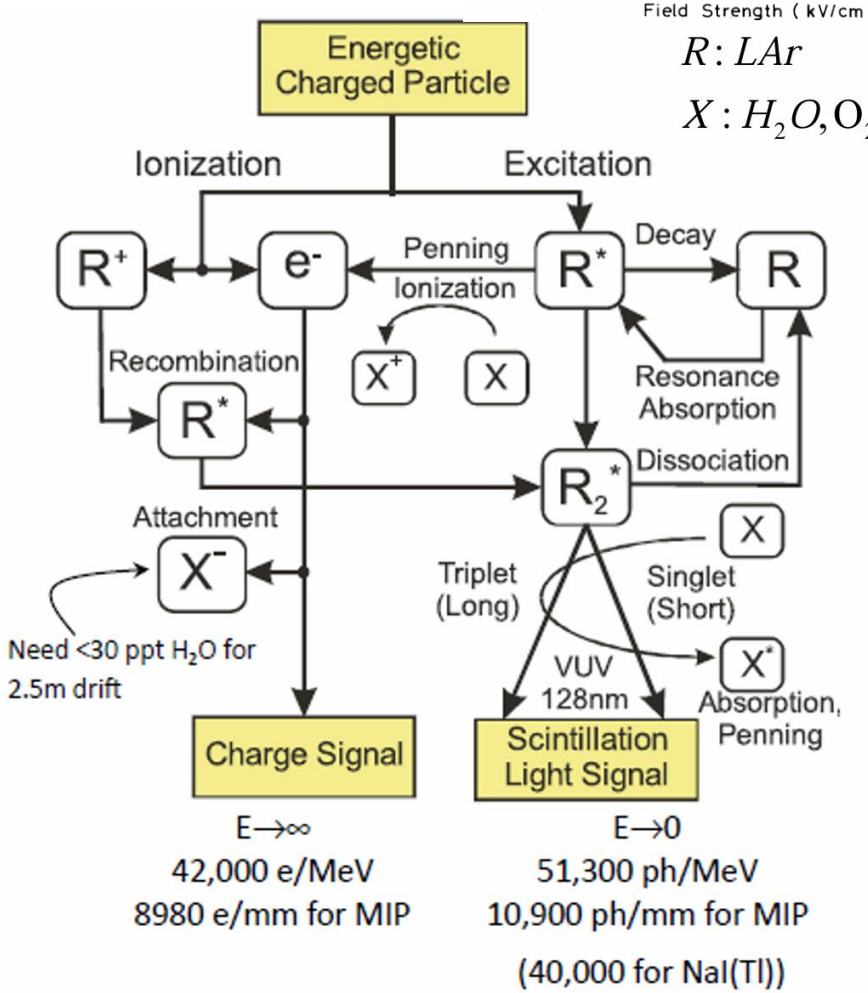

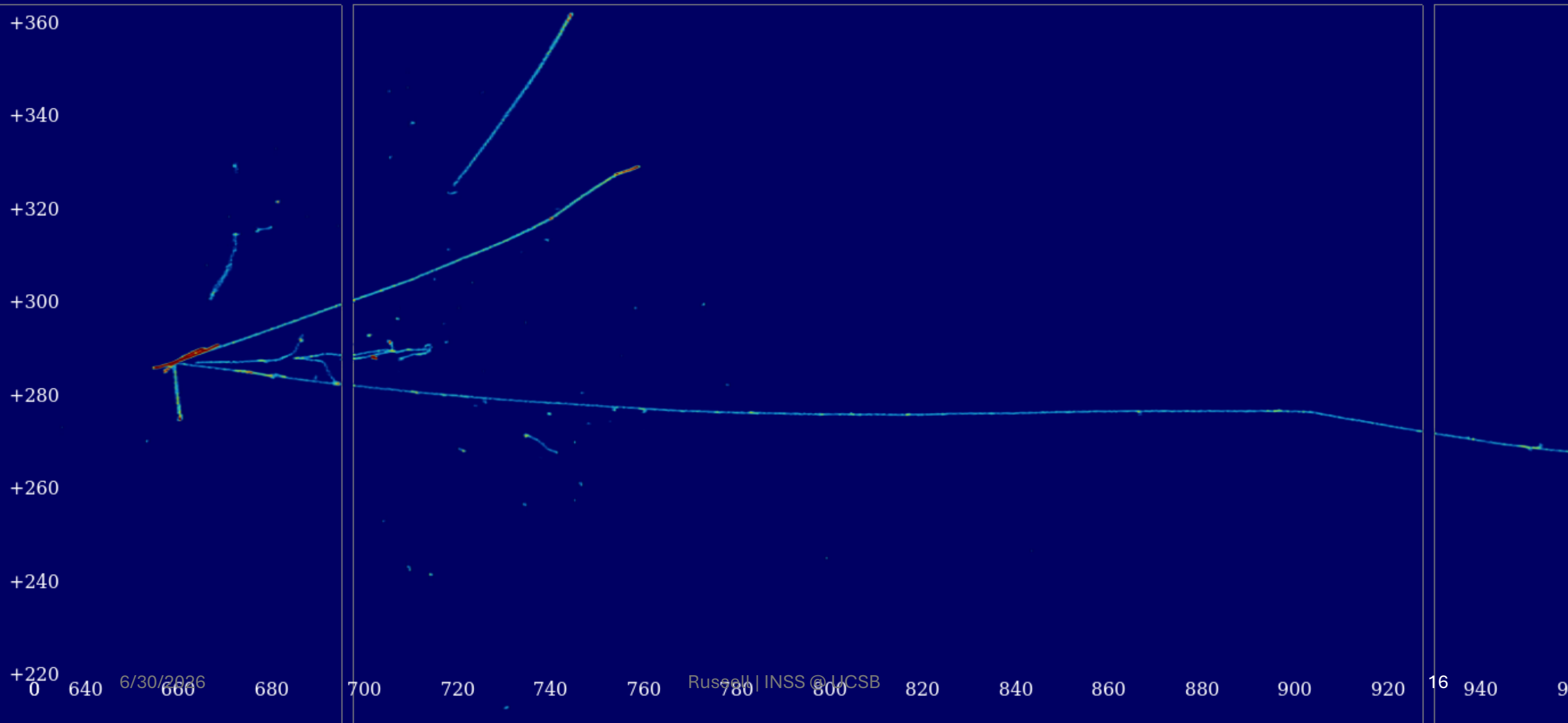
+360
+340
+320
+300
+280
+260
+240
+220
0
640
660
680
700
720
740
760
780
800
820
840
860
880
900
920
940

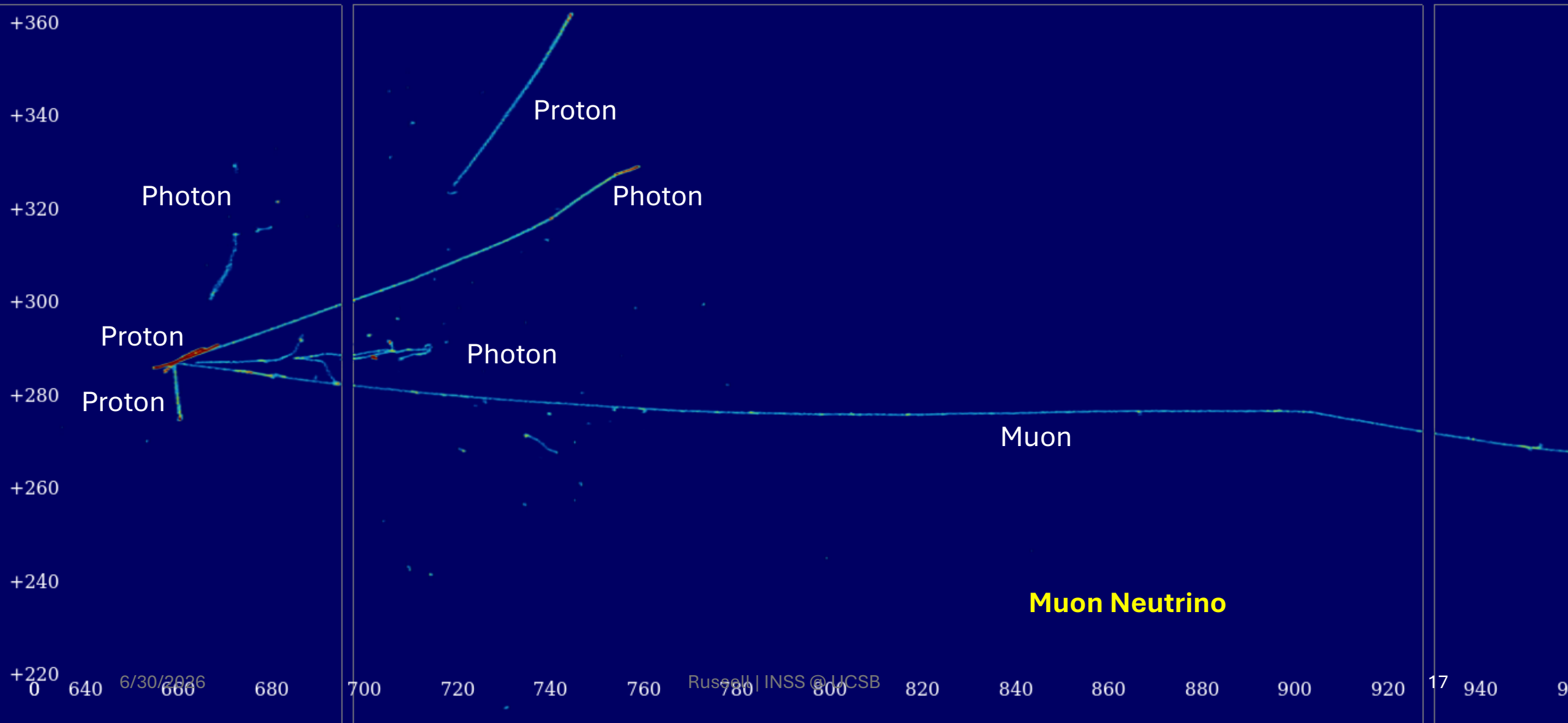
+360
+340
+320
+300
+280
+260
+240
+220
0
640
660
680
700
720
740
760
780
800
820
840
860
880
900
920
940
Proton
Photon
Photon
Proton
Photon
Proton
Muon
Muon Neutrino

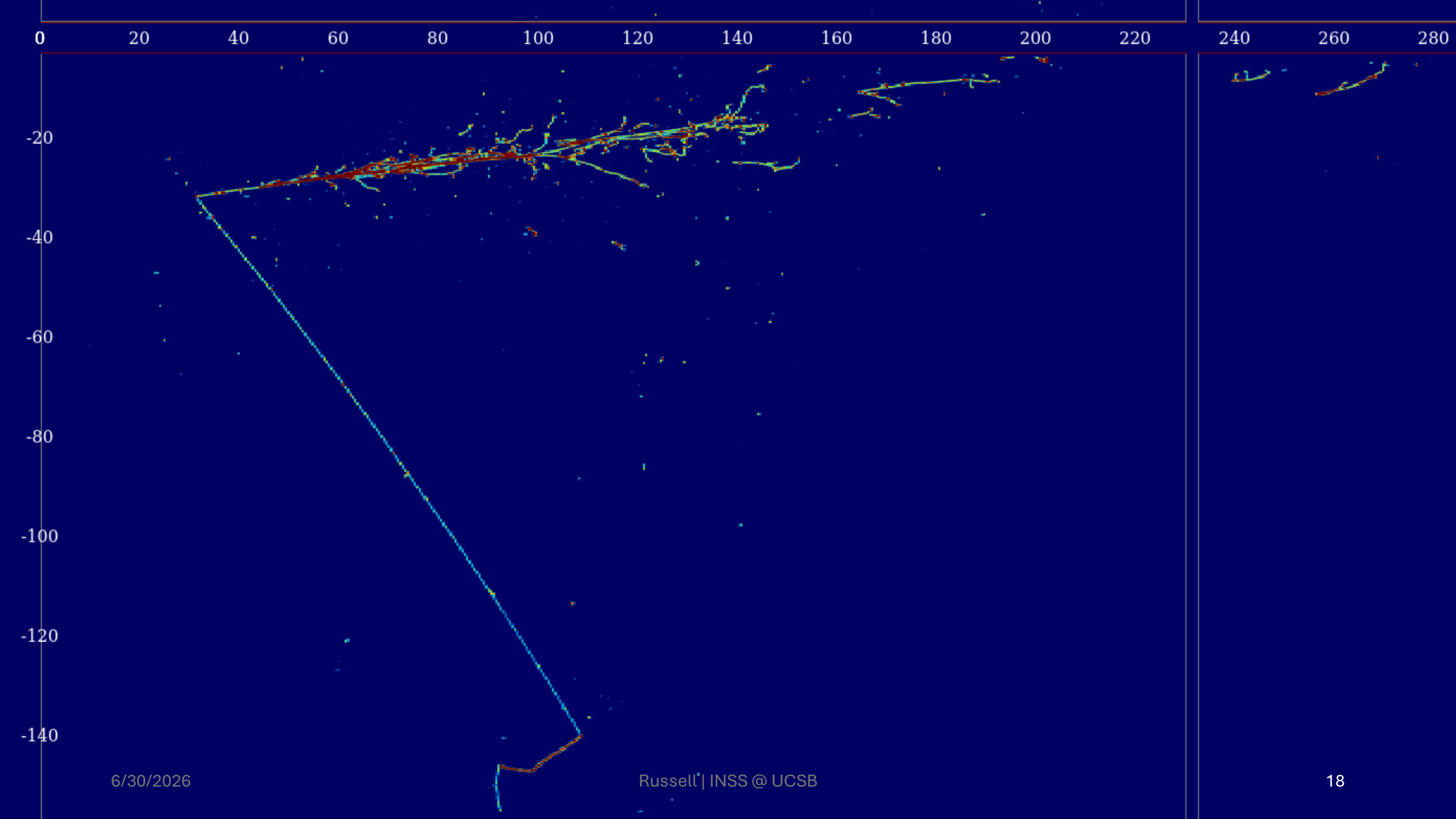
0
20
40
60
80
100
120
140
160
180
200
220
240
260
280
-20
-40
-60
-80
-100
-120
-140

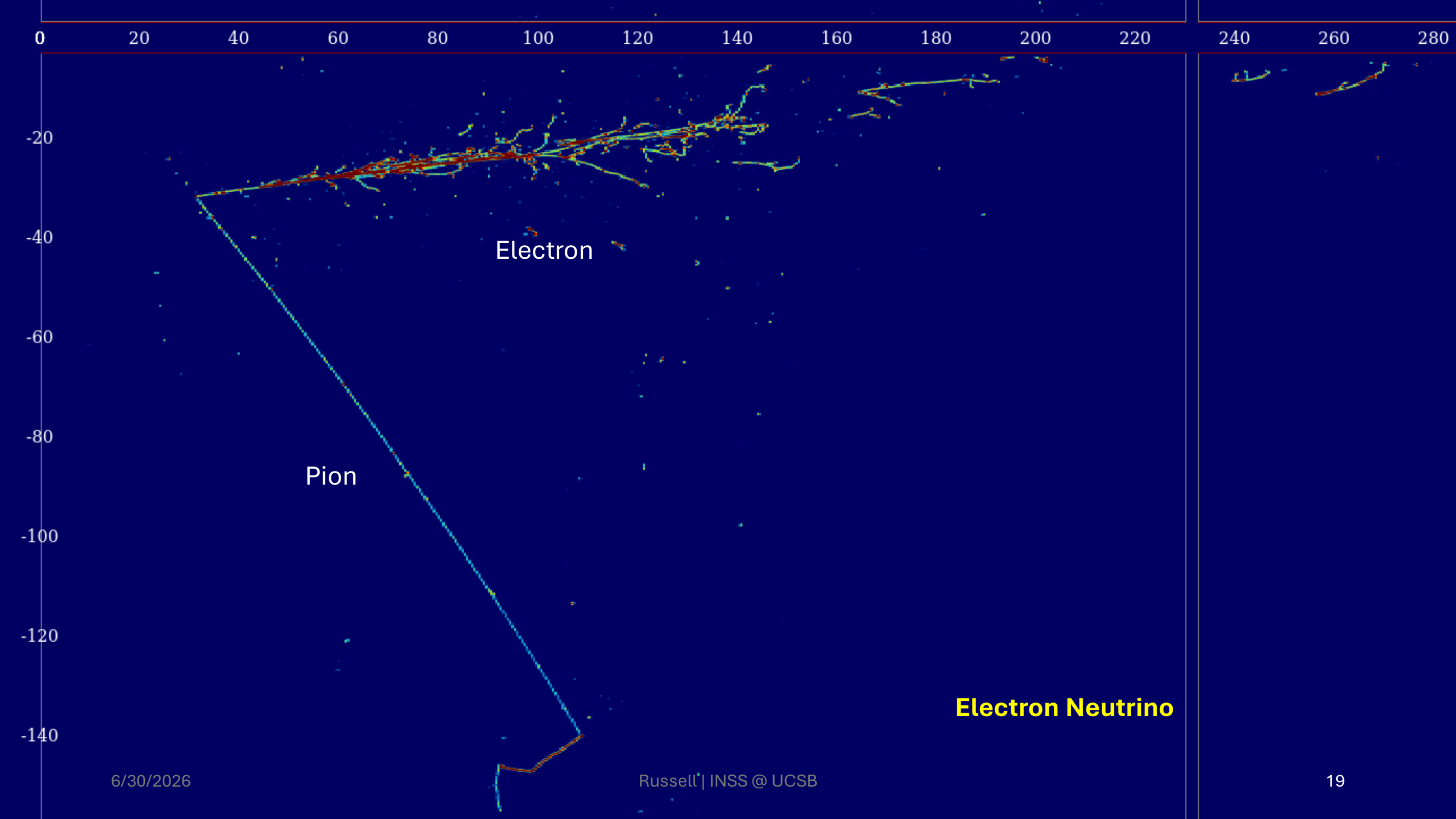
0
20
40
60
80
100
120
140
160
180
200
220
240
260
280
-20
-40
-60
-80
-100
-120
-140
Electron
Pion
Electron Neutrino

Projective Readout Signal Processing Development I

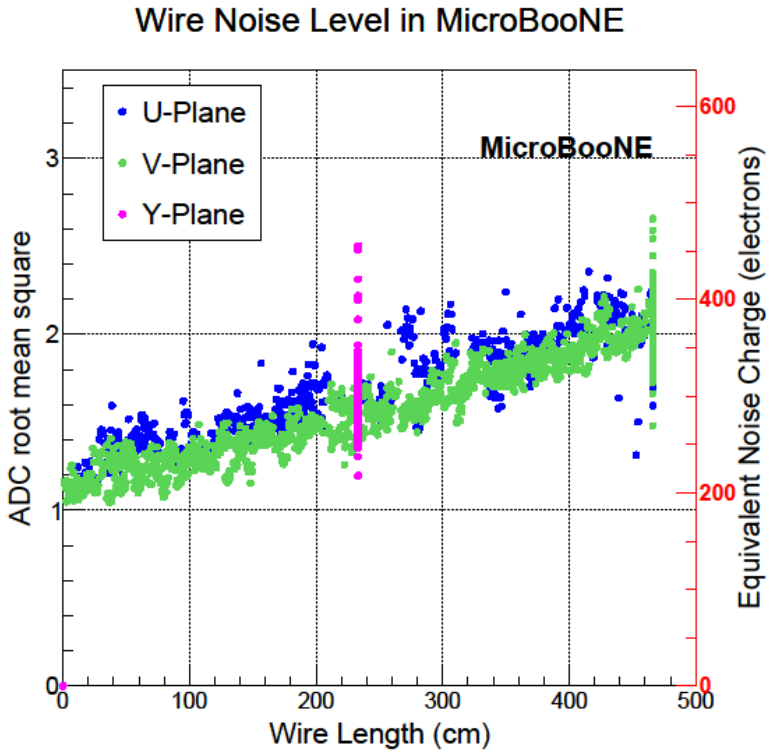

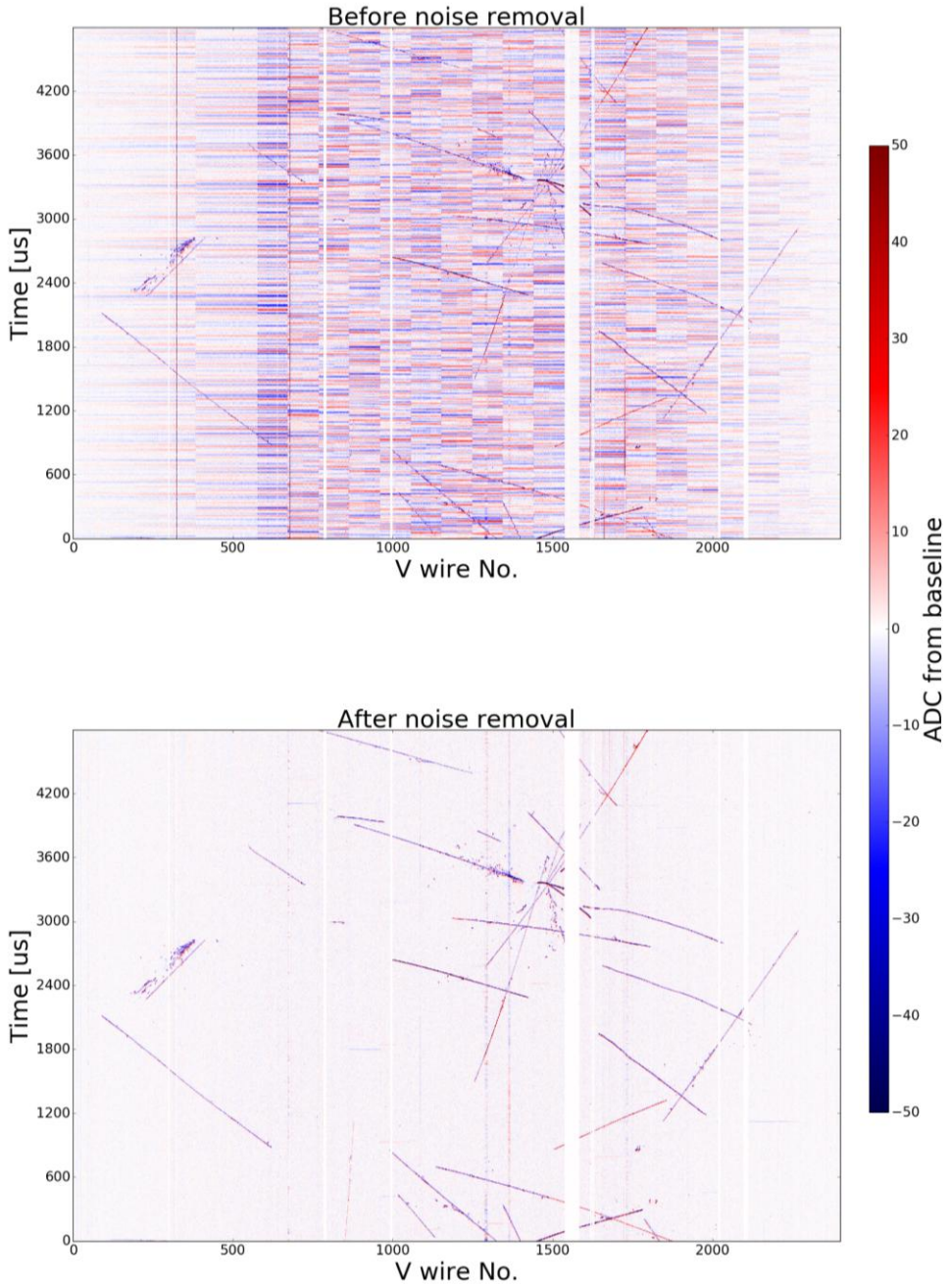

- Demonstrated low inherent electronics noise
- Excess noise mitigation

JINST **12** P08003 (2017)

Induced Current on Charge-Sensitive Electrodes

Governed by the Shockley-Ramo theorem:

$$i = -q\vec{E}_W \cdot \vec{v}_q$$

Consequently, measured charge from charge q_m moving along a drift path:

$$\int i\, dt = q_m \cdot (V_w^{end} - V_w^{start})$$

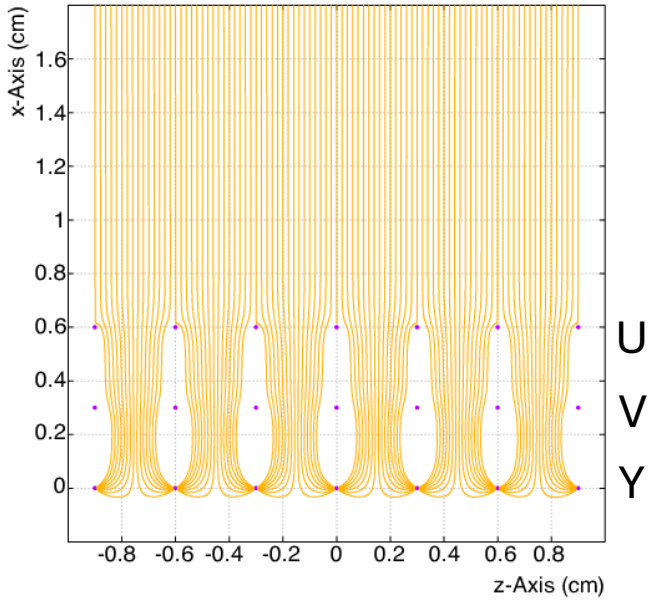

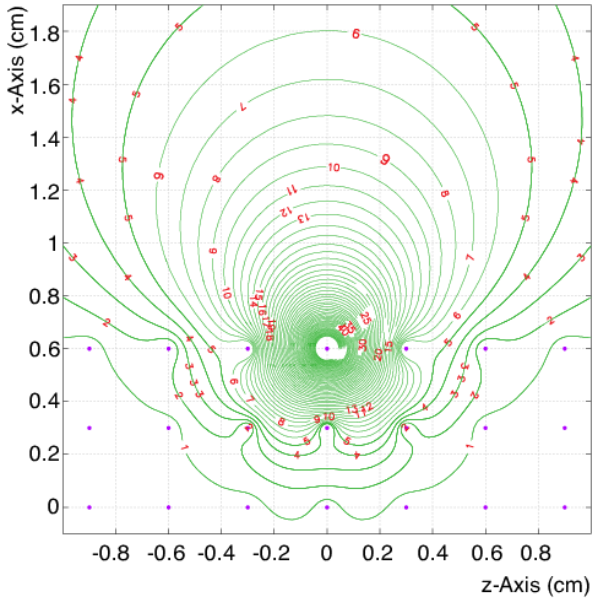

1st induction (U plane)

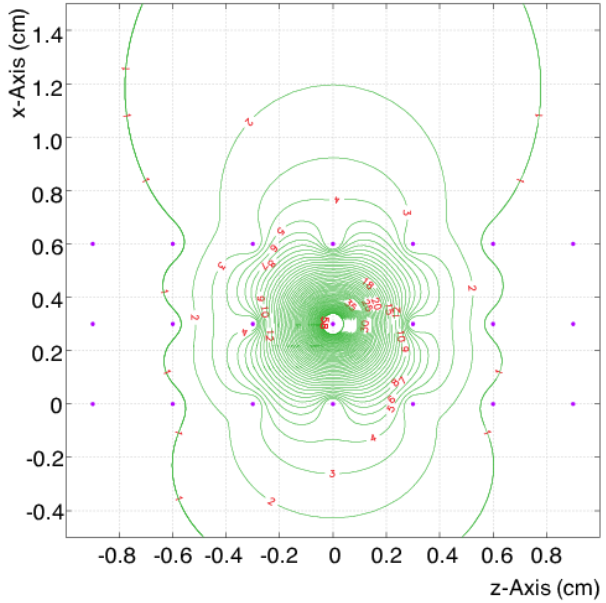

2nd induction (V plane)

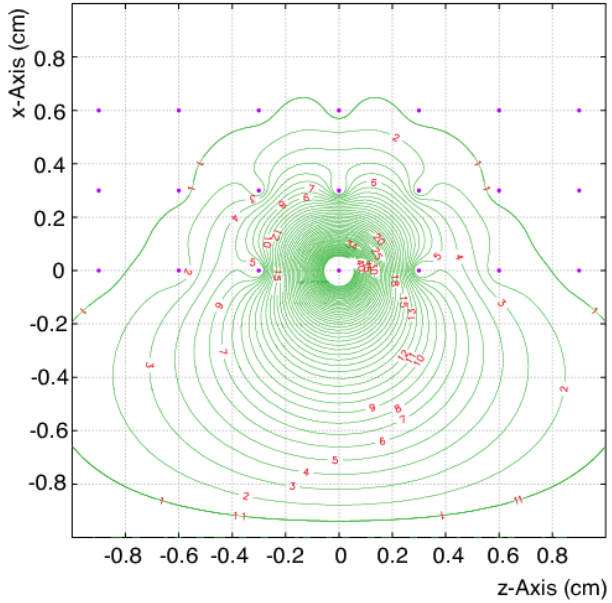

collection (Y plane)

Signal Detection in LArTPCs

LArTPC charge sensors measure the *coherent sum of induced currents from the totality of the ionization charge profile*

Beware: subtle topology dependencies and artifacts!

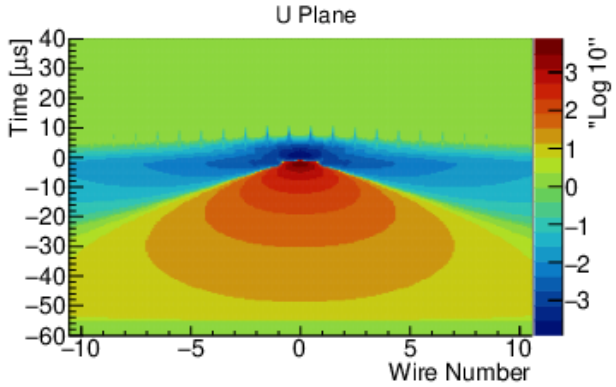

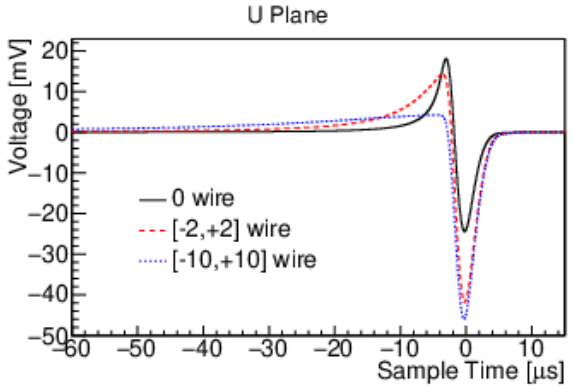

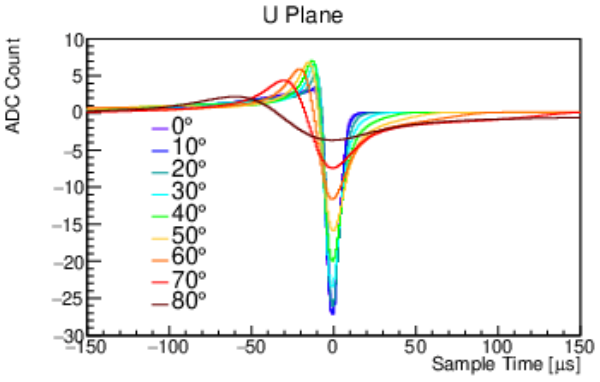

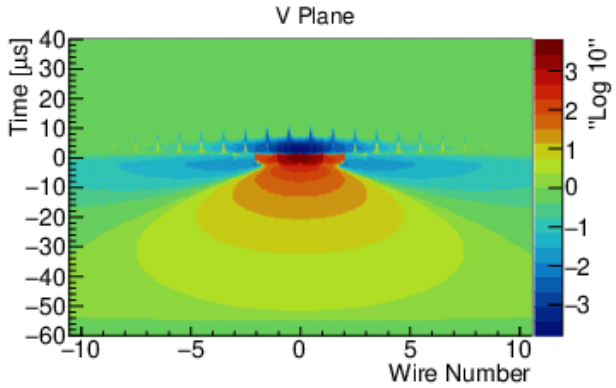

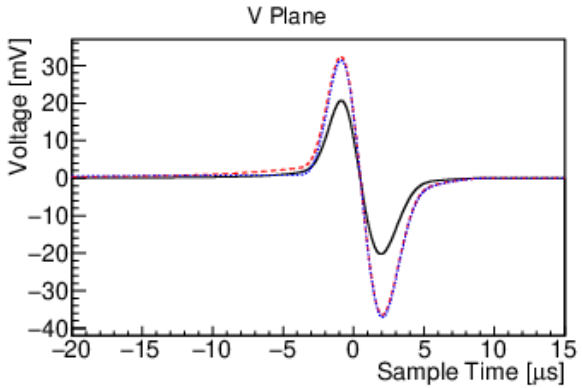

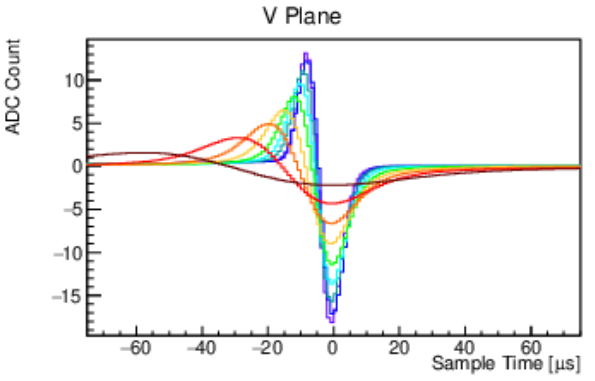

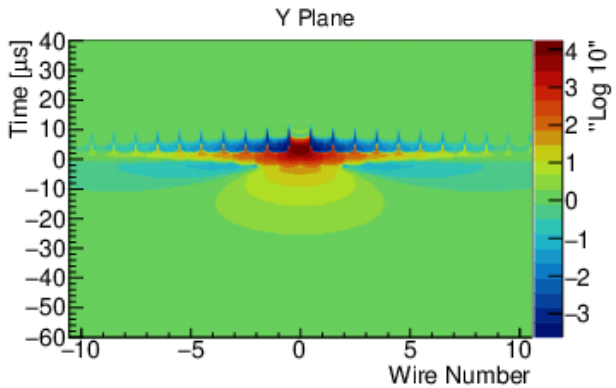

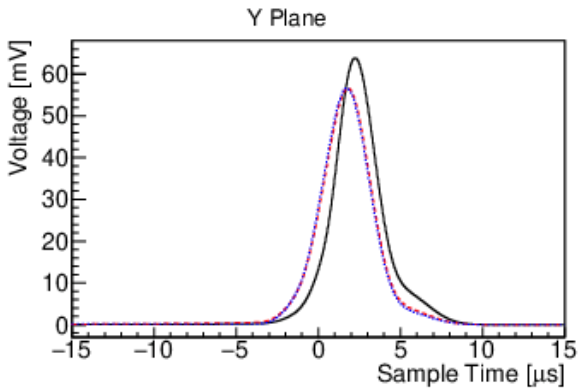

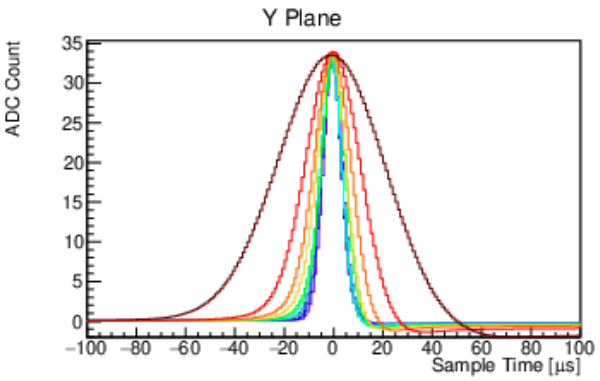

Projective Readout Signal Processing Development II

The measured signal on a single wire

$$M_i(t_0) = \int_t R_0(t - t_0) \cdot S_i(t) + R_1(t - t_0) \cdot S_{i+1}(t) + \cdots) \cdot dt$$

where R_i is an average response and S_i is the true signal

By applying a Fourier transform

$$M_i(\omega) = R_0(\omega) \cdot S_i(\omega) + R_1(\omega) \cdot S_{i+1}(\omega) + \cdots$$

We can invert to solve directly for the true charge

$$S(\omega) = \frac{M(\omega)}{R(\omega)} \cdot F(\omega)$$

where a filter function $F(\omega)$ is added to attenuate noise

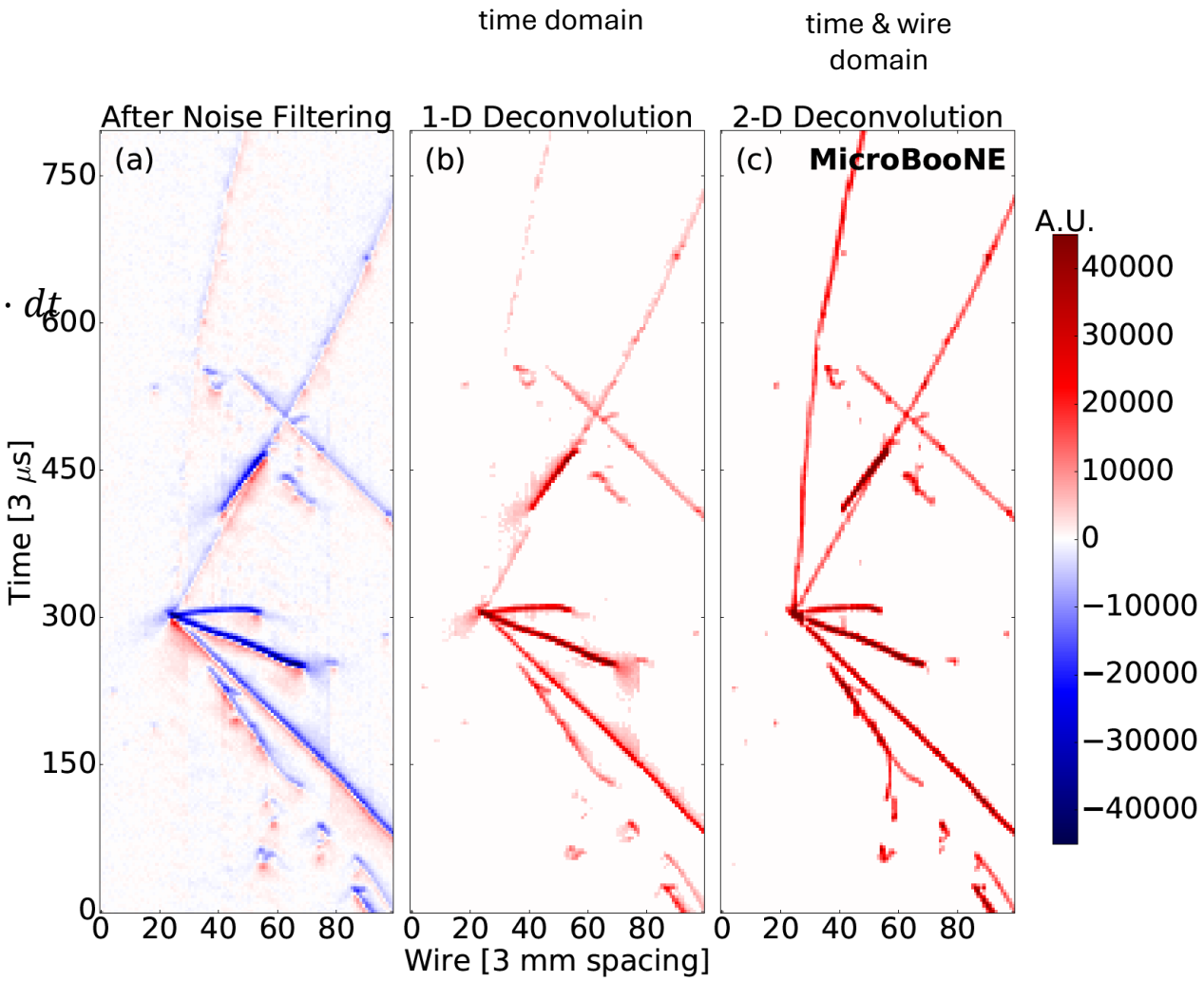

Improved understanding of detector response

JINST **13** P07006 (2018)

MicroBooNE first demonstrated of charge matching across planes

Critical for accessing robust **calorimetric** & **topological** information for downstream reconstruction

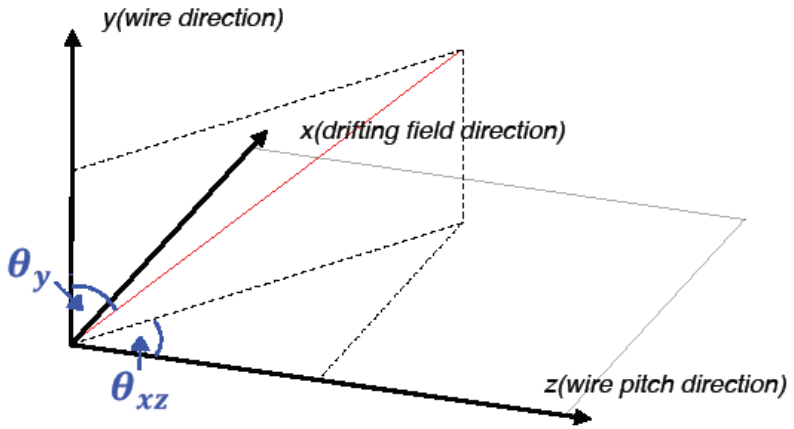

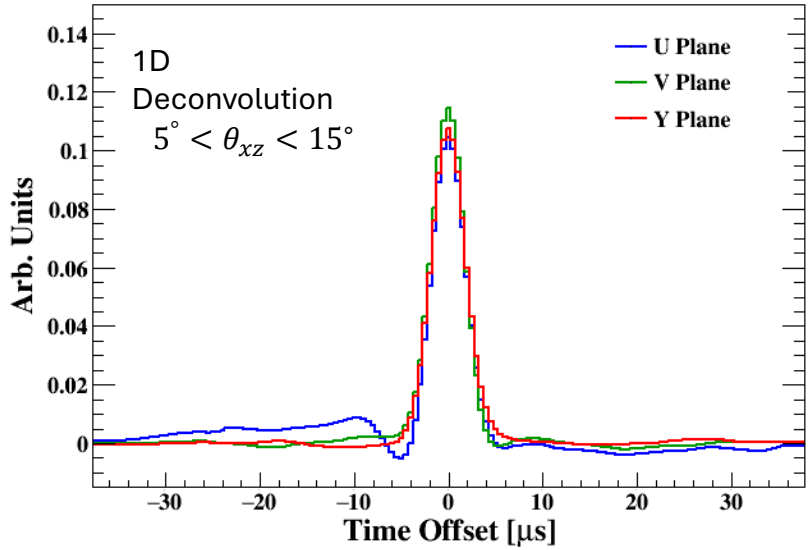

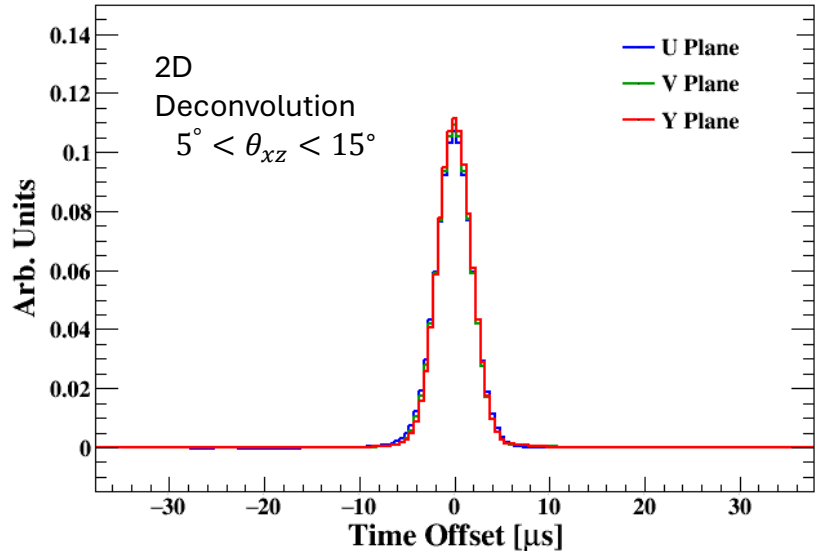

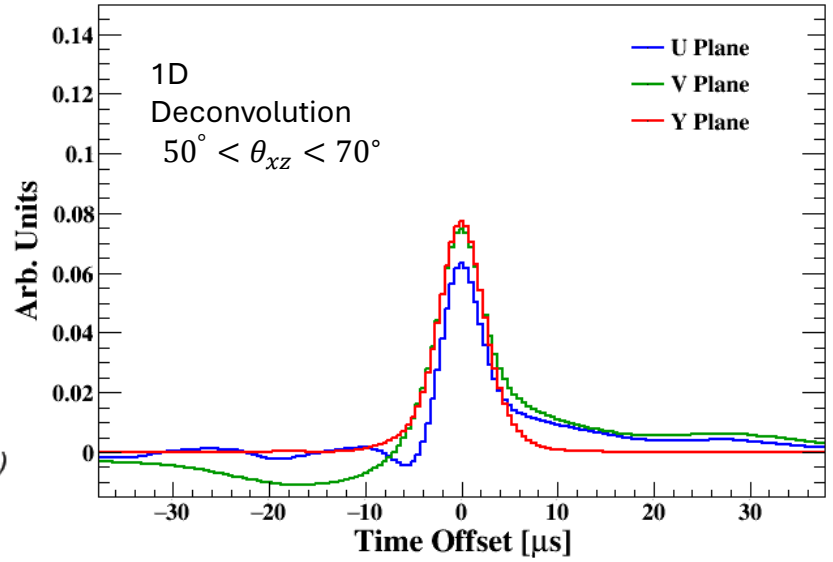

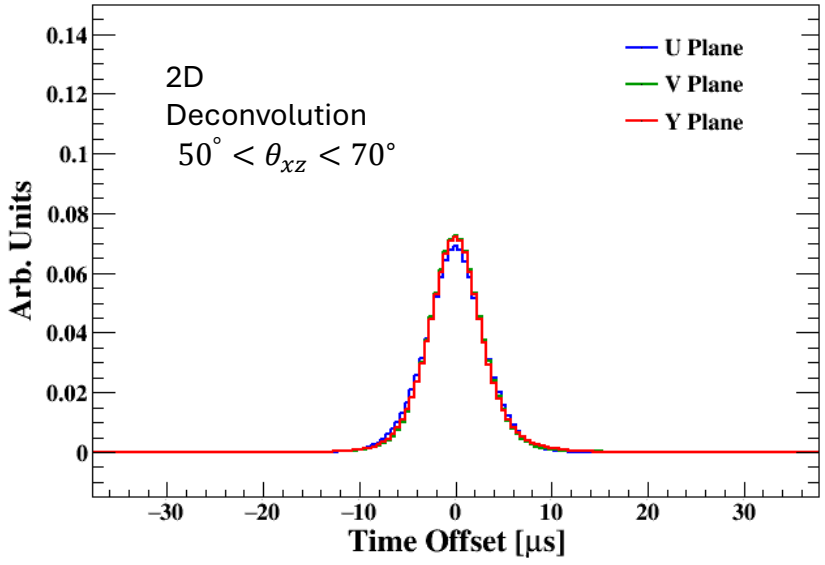

Far Detector

40 kilotonne liquid Argon time-projection chamber detectors located one mile underground in Lead, SD

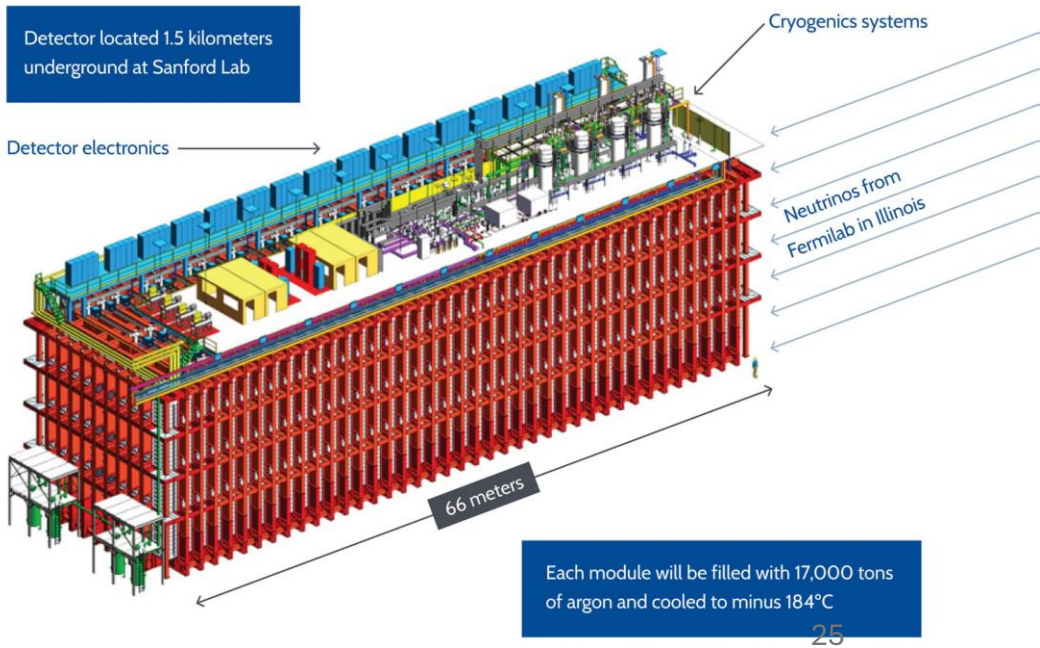

DUNE Vertical Drift Far Detector Charge Sensing

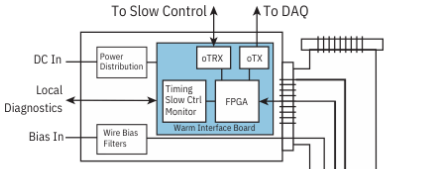

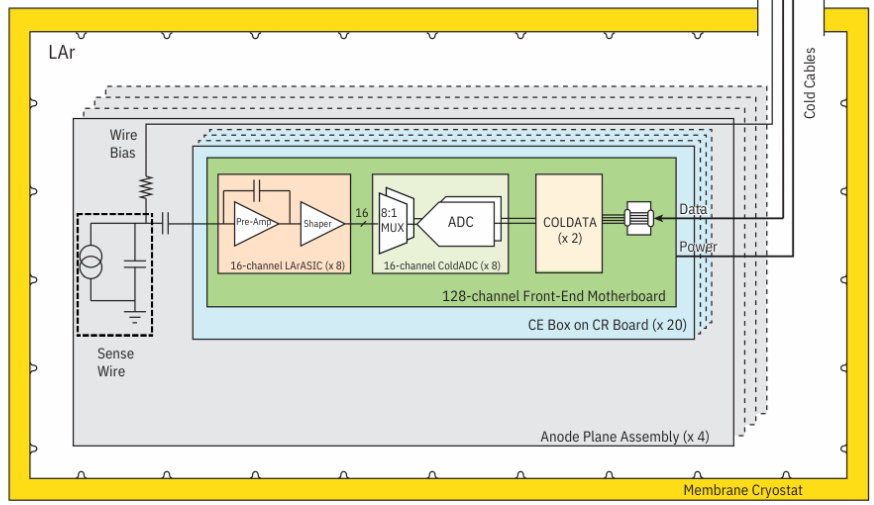

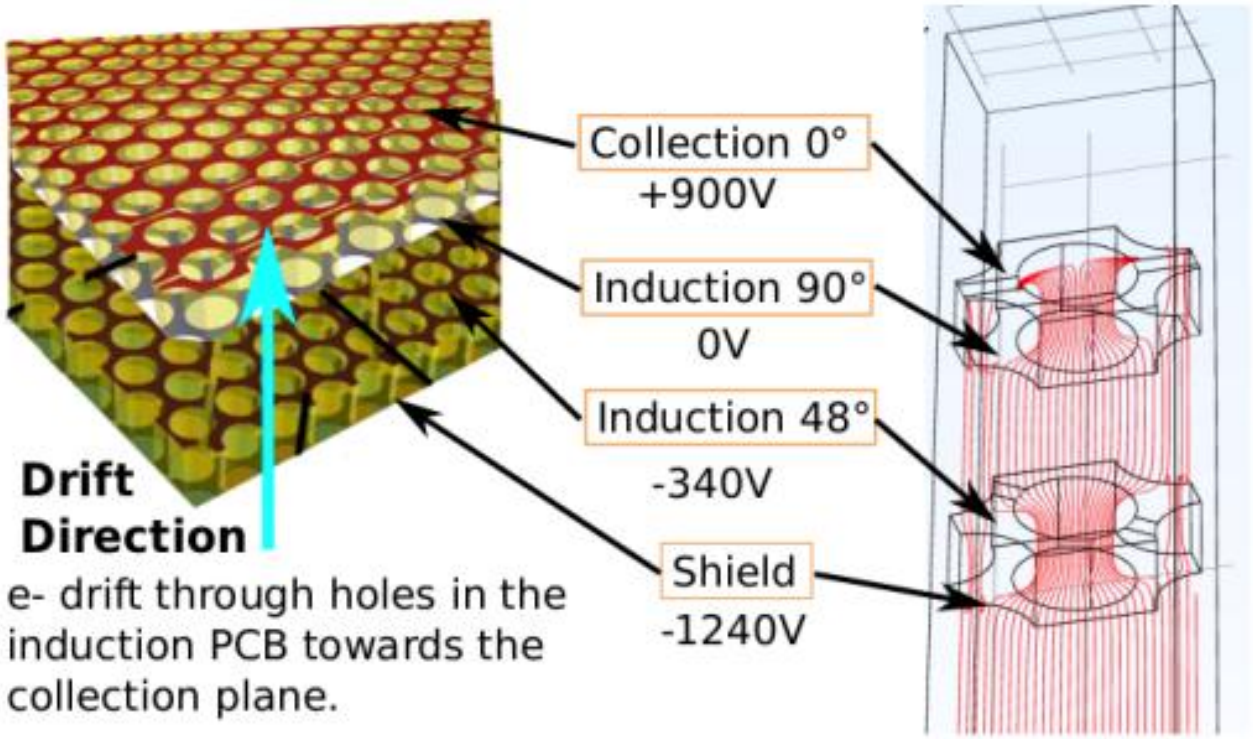

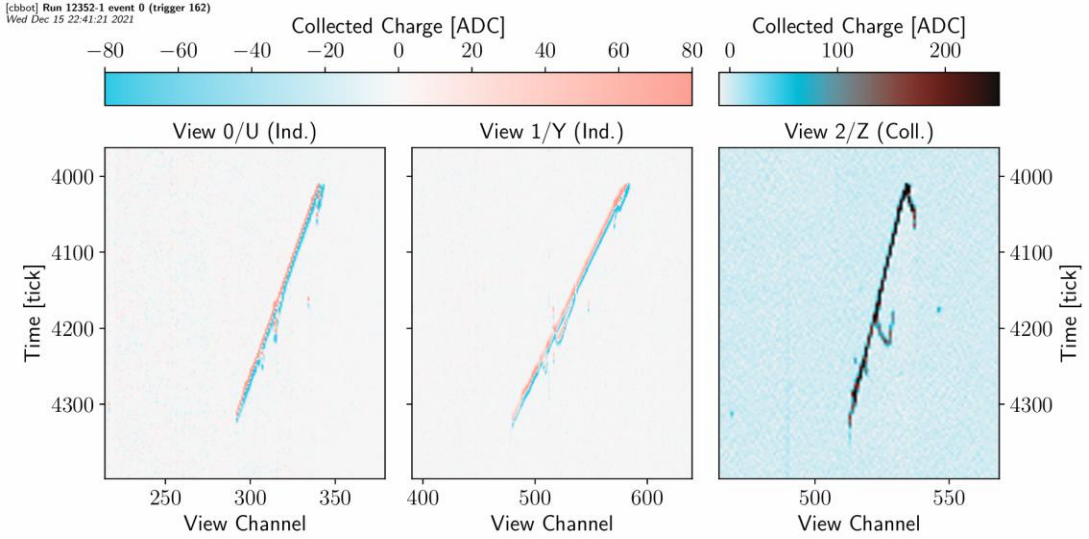

DUNE Vertical Drift Far Detector Light Sensing

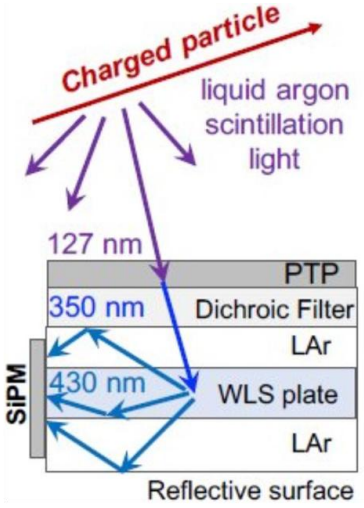

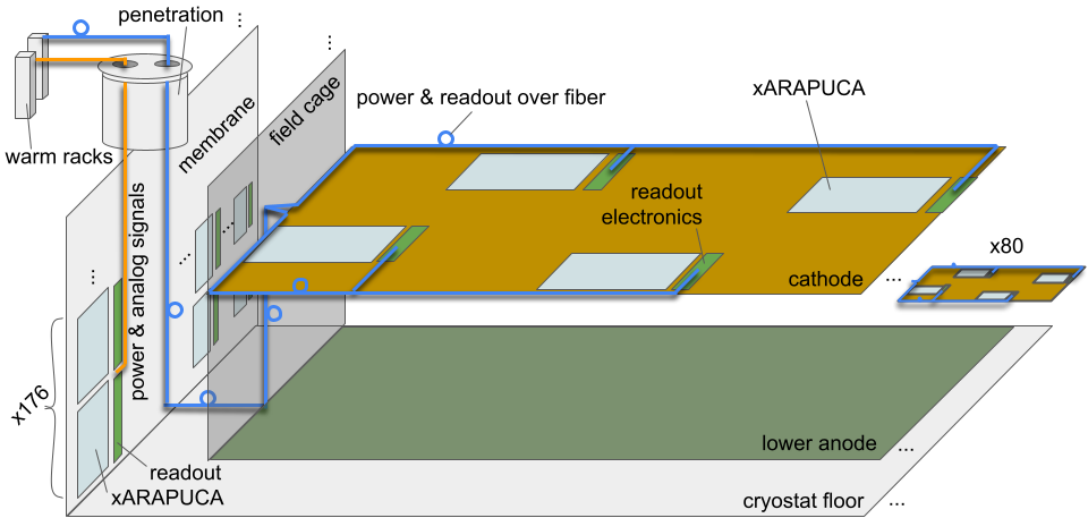

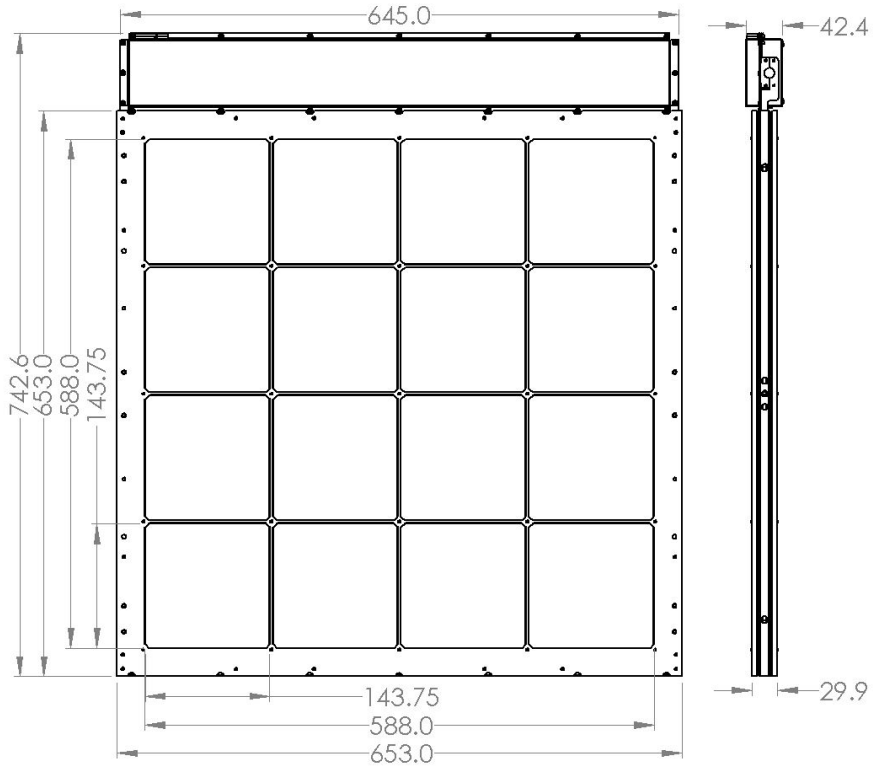

DUNE LArTPC Ionization Sensing

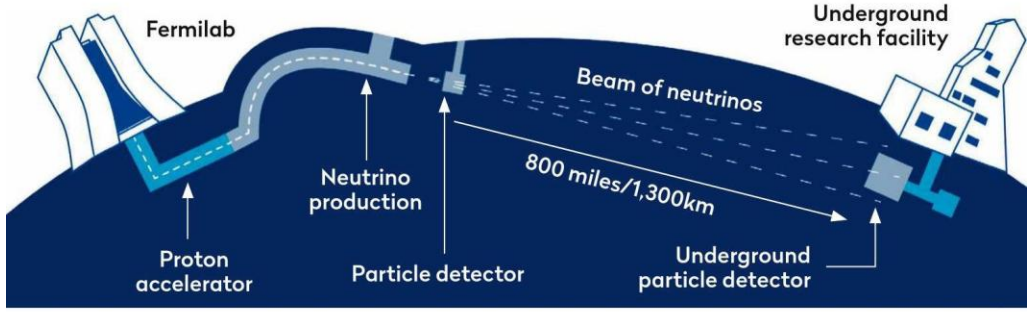

Projective readout (strips or wires):
native 2D --> 3D

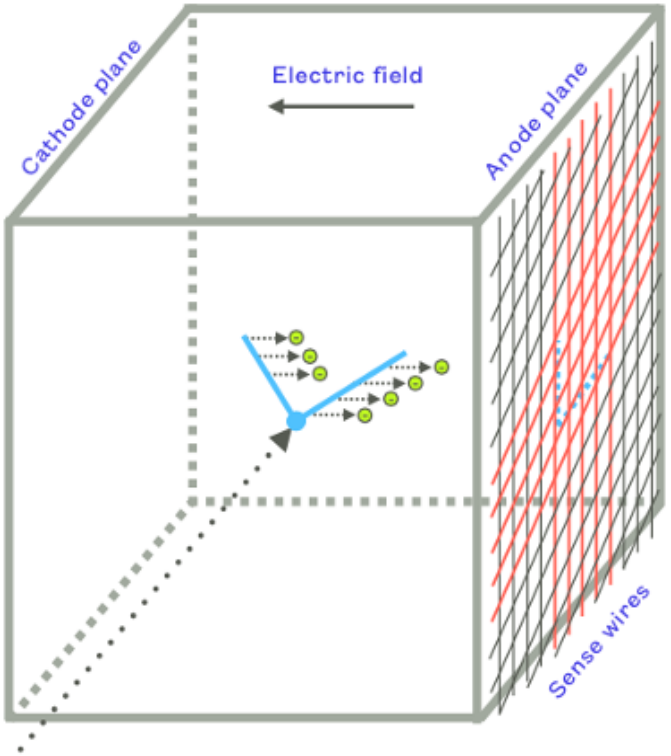

- Forced trigger with continuous sampling
- Sense plane position is topology dependent, indeterminate with single plane
- Multiple redundant charge measurements

Far detector 1 & 2 technology

Pixelated readout:
inherently 3D

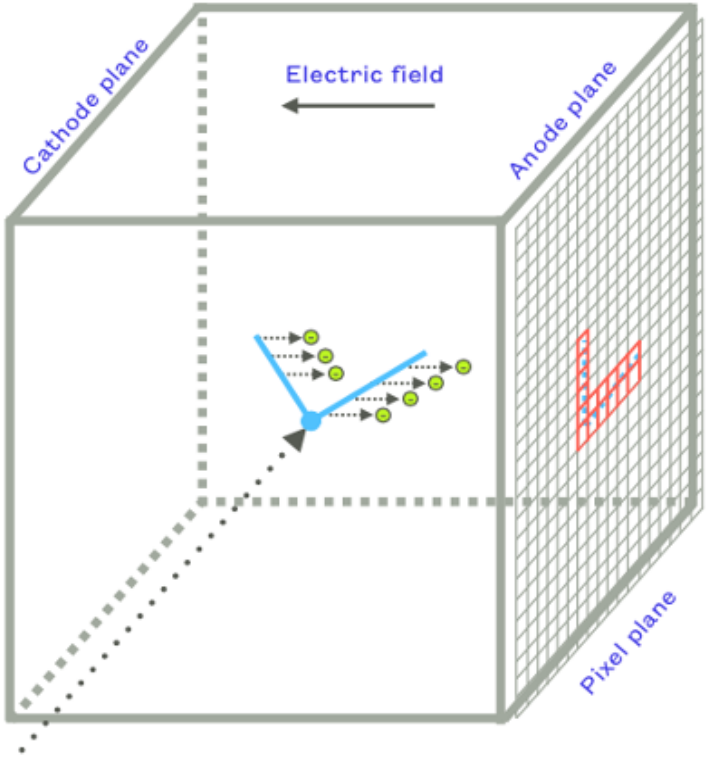

- Zero-suppressed, self-trigger
- Sense plane position is absolute
- Sub-threshold charge is irrecoverable
- Single measurement

Near detector technology & proposed far detector 3

DUNE Near Detector Complex

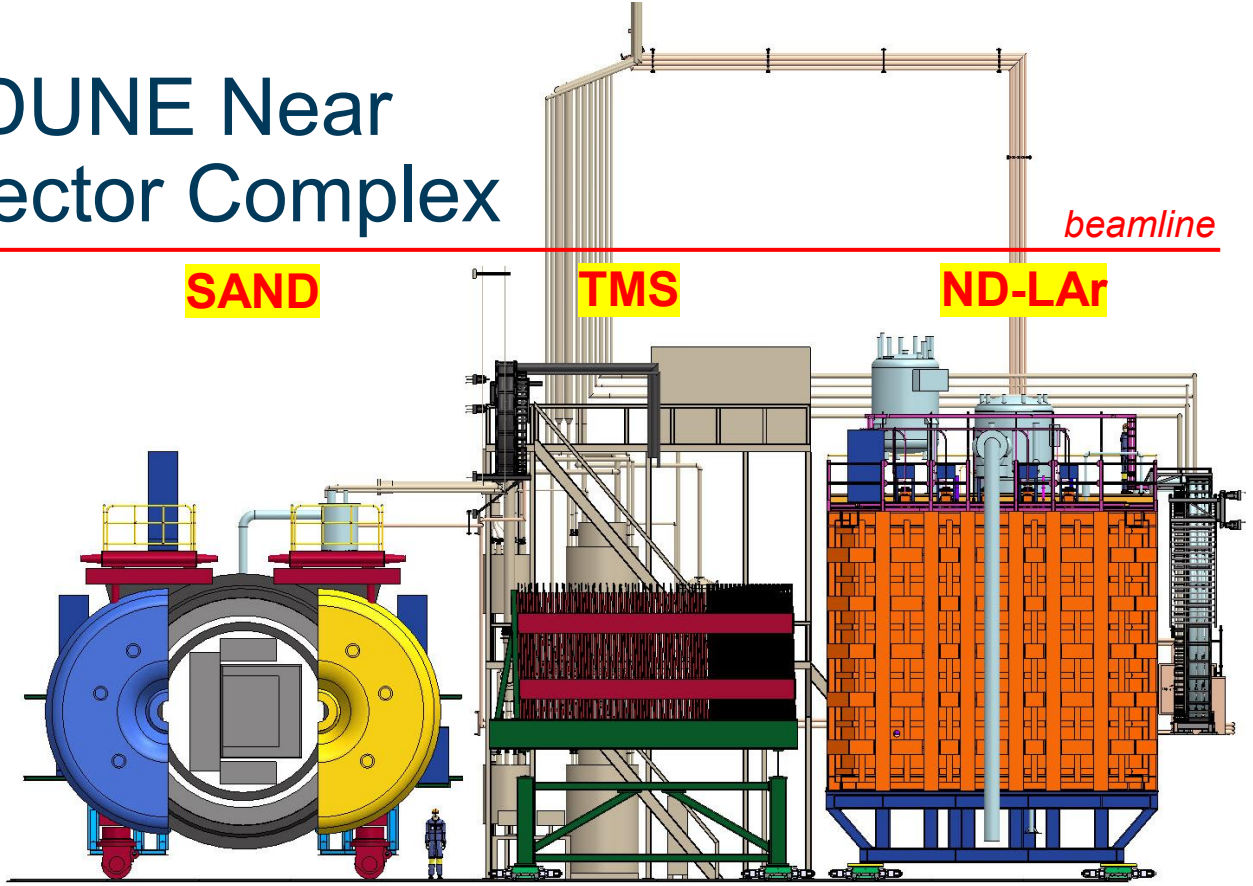

Precision Reaction-Independent Spectrum Measurement (PRISM)

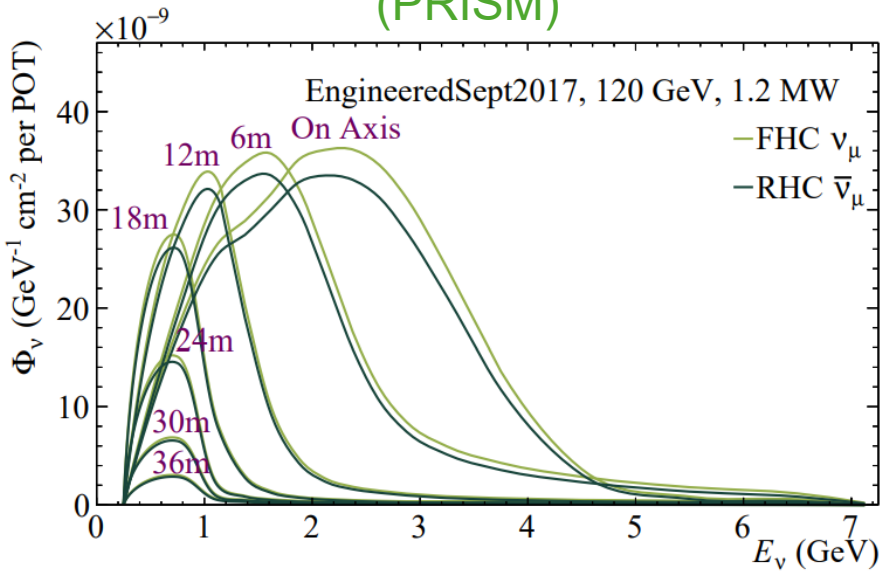

Far detector appearance signal:

$$\frac{dN^{far}_{\nu_{e-CC}}}{dE_{rec}} = \int_{E_\nu} D^{far}_{\nu_e-CC}(E_{rec};E_\nu)\,\sigma^{Ar}_{\nu_e-CC}(E_\nu)\,P_{\mu e}(E_\nu)\,\Phi^{far}_{\nu_\mu}(E_\nu)\;dE_\nu$$

constrained by detector model

constrained by theory

constrained by beam model and near detector data

Near detector signal:

$$\frac{dN^{near}_{\nu_\mu-CC}}{dE_{rec}} = \int_{E_\nu} D^{near}_{\nu_\mu-CC}(E_{rec};E_\nu)\,\sigma^{Ar}_{\nu_\mu-CC}(E_\nu)\,\Phi^{near}_{\nu_\mu}(E_\nu,d)\times w\;dE_\nu$$

Off-axis ND-LAr/TMS for data-driven *oscillated FD flux* prediction

Beam-neutrino pileup: an unprecedented experimental regime

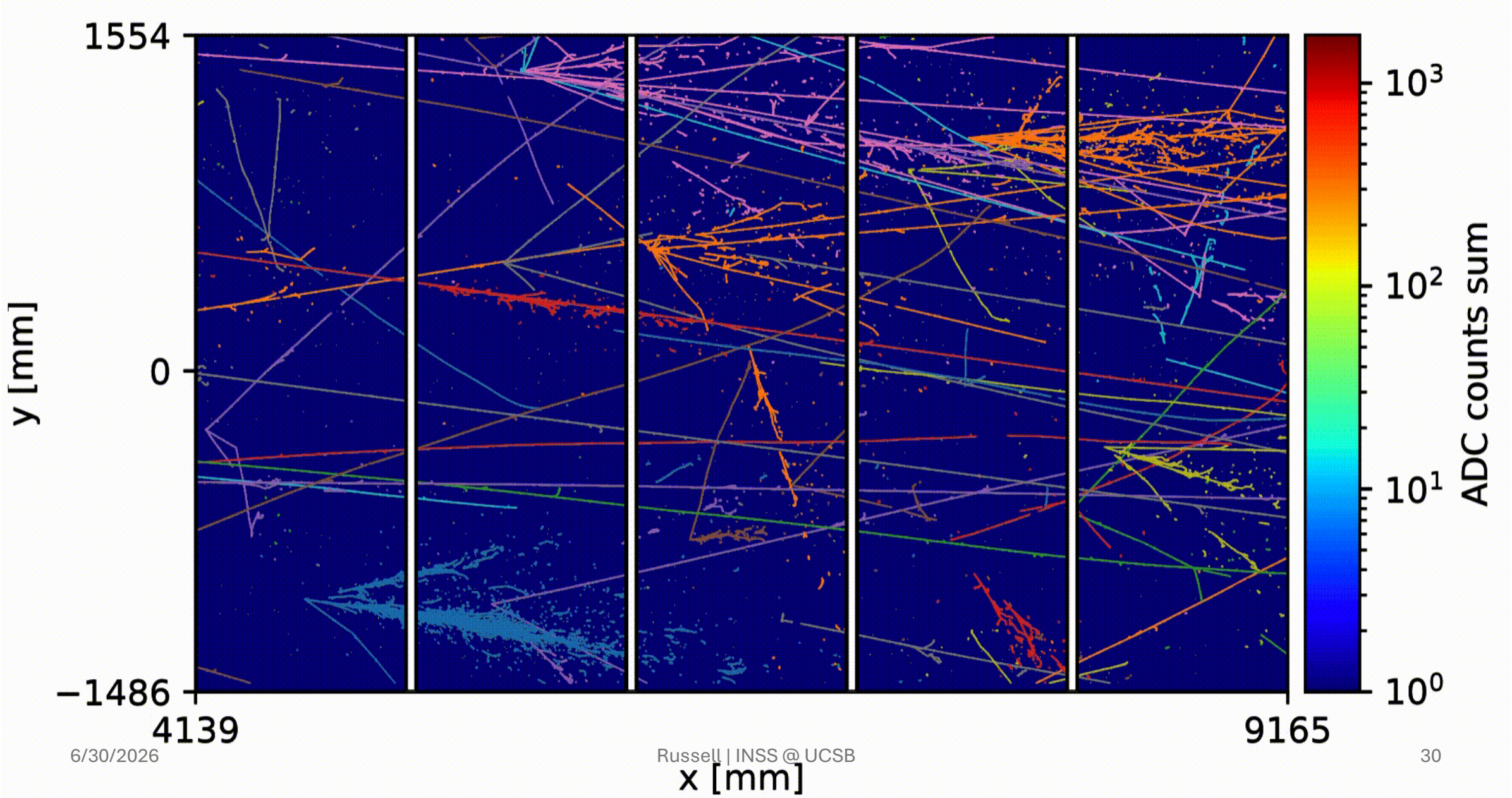

Module Design *a next-generation LArTPC*

Key design driver: maintain signal fidelity in high occupancy environment (beam ν pileup!)

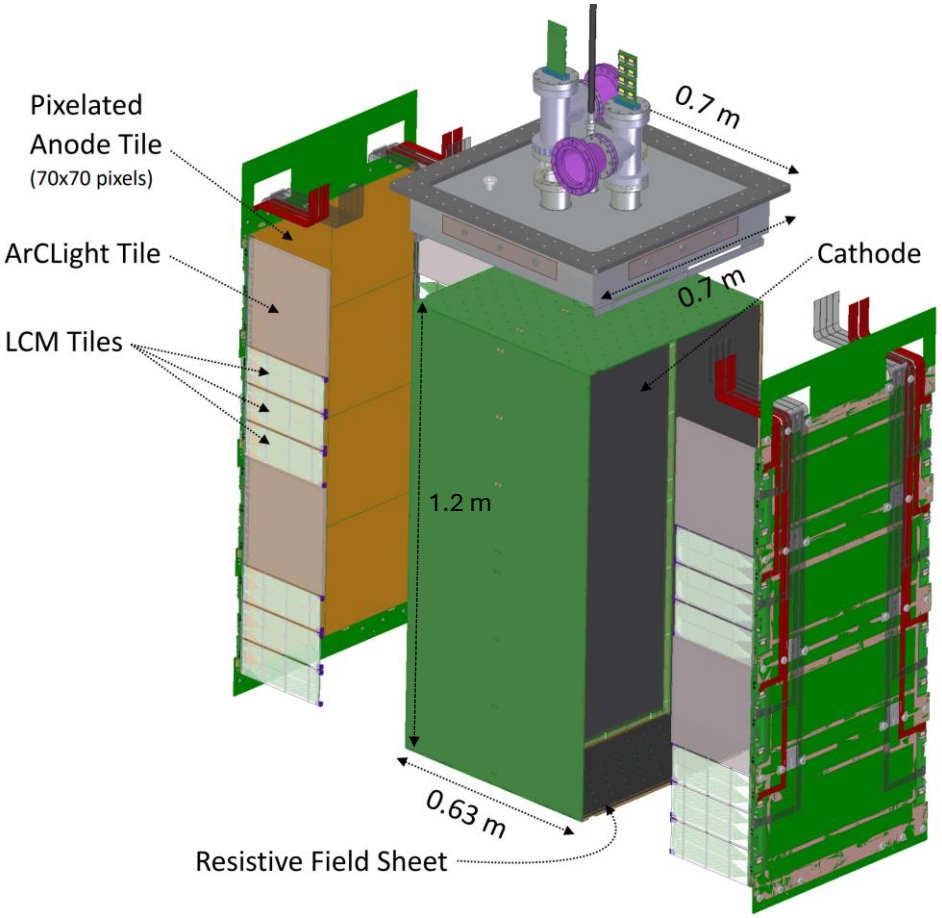

60%-scale ND-LAr module prototype

- **Optical segmentation**
- - Contained scintillation light to mitigate ν pileup
- **Modular TPCs**
- - Potential failures contained to finite sub-region
- **Short charge drift distance**

•- Reduce requirements/risks associated with HV, purity, and field uniformity

- **Low-profile field cage**
- - Reduce inactive volumes
- **High-photocoverage light readout**
- - ν pileup mitigation with ~10 cm spatial resolution and < 10 ns timing resolution
- **Pixelated charge readout**

•- ν pileup mitigation with true 3D readout

•- Reduced sensitivity to system noise

•- Scalable, mechanically robust, commercially produced PCB design

Motivation for pixelated charge readout

3D charge reconstruction ambiguity is a natural consequence of projective readout with wire geometry

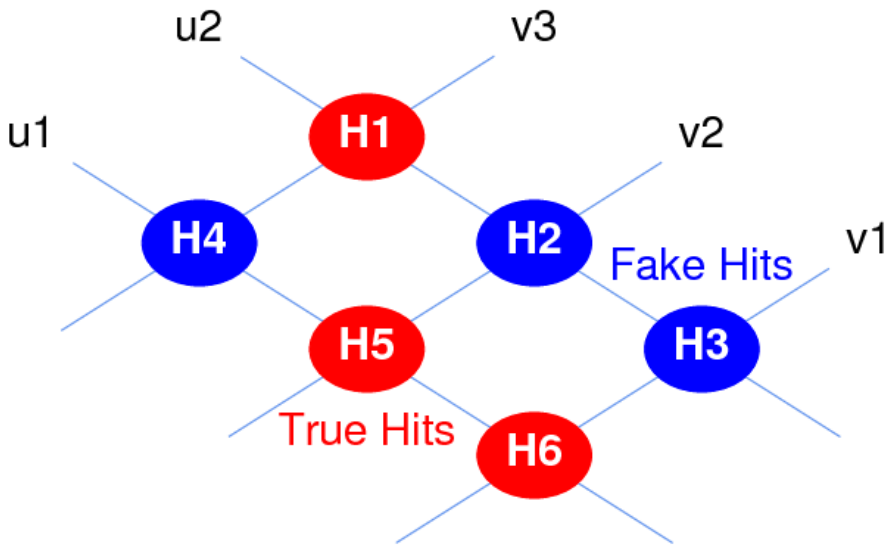

Truth

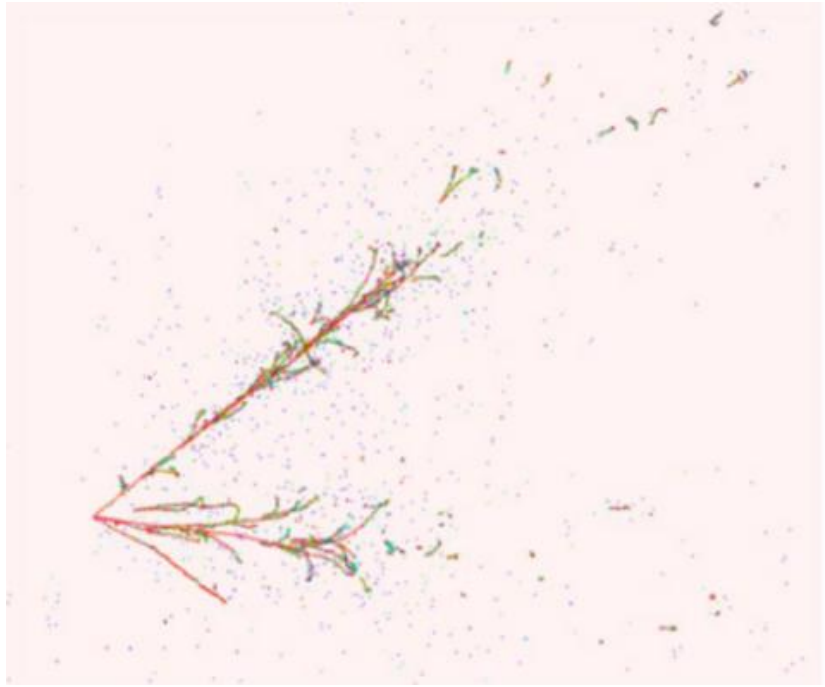

Reconstruction with wire readout

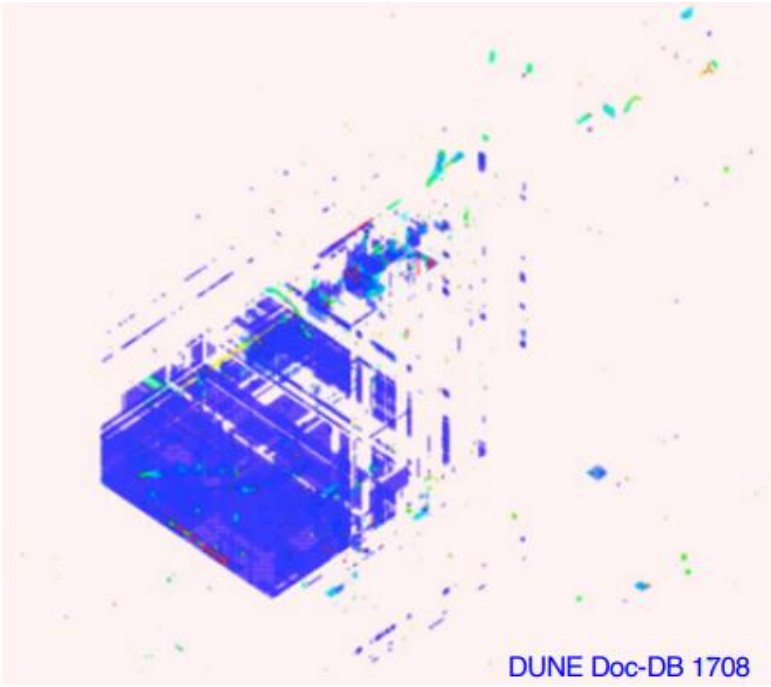

LArPix Charge Readout System-level Design

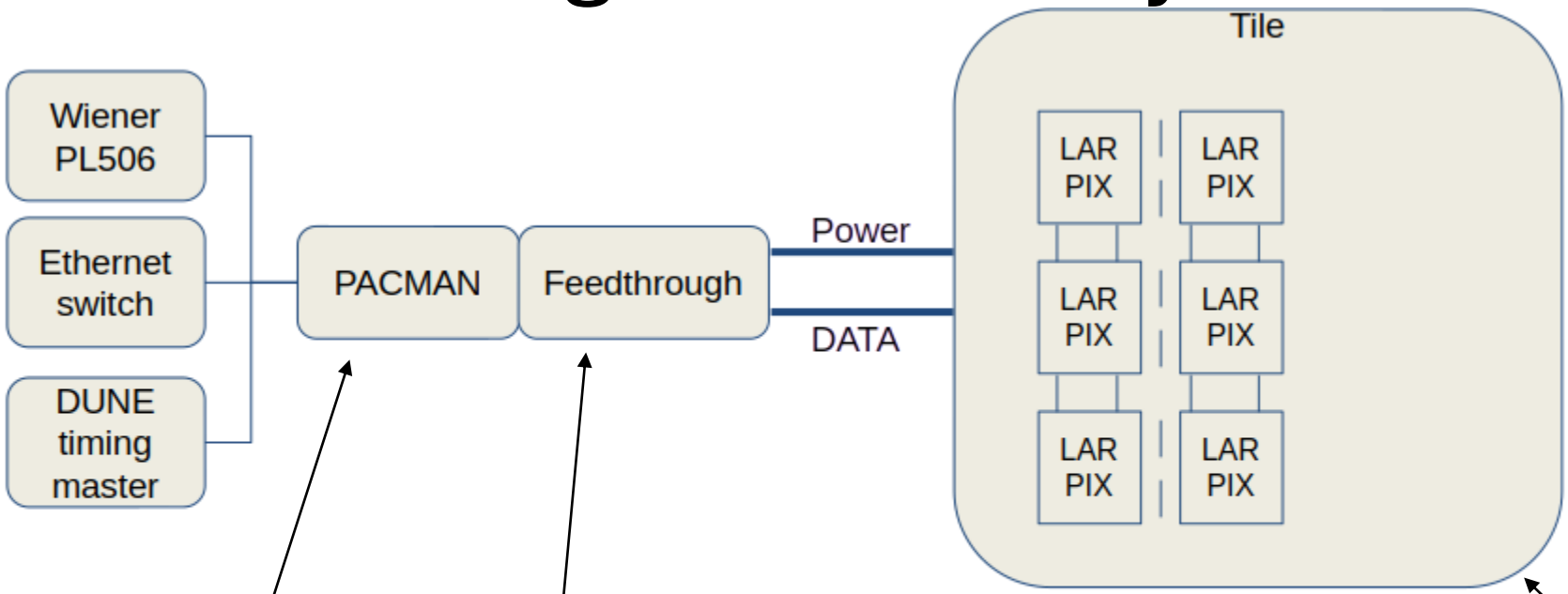

LArPix Hydra network enables redundant data transport on and off tile. No single point of failure.

Distributed data buffer minimizes throughput requirements.

Network topology can be chosen to minimize buffer usage or latency.

COTS or externally supplied

Low voltage, low complexity design, use of COTS FPGA module

Passive, low complexity PCB

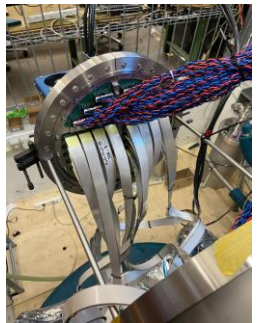

Low data rate enables use of simple ffc cables

Standard PCB technology leverages industry pricing, production, assembly capability

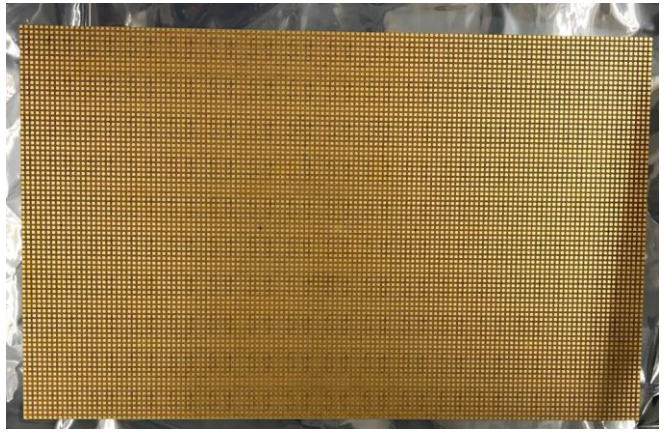

LArPix-v3 ASIC Overview

Cryo-compatible, low-power mixed-signal ASIC (TSMC 130 nm) designed for pixelated, true 3D readout of LArTPC detectors

Continuous self-triggered pixelated free streaming readout, ~100% uptime

Principal component of the end-to-end LArPix readout system: \$0.10/channel (\$10k/m^2)

Specification	Value
Analog Inputs	64
Gain	3.4 μV/e-
Noise	350 ENC
Power	<170 μW/channel
Dynamic Range	340 ke-
AFE Settling Time	<200 ns
Minimum Resampling Time	1.4 μs
Timestamp Precision	100 ns
Linearity	0.9%
ADC Resolution	10 bits
Operating Temperature	77 K to 300 K

LArPix Analog Front-End

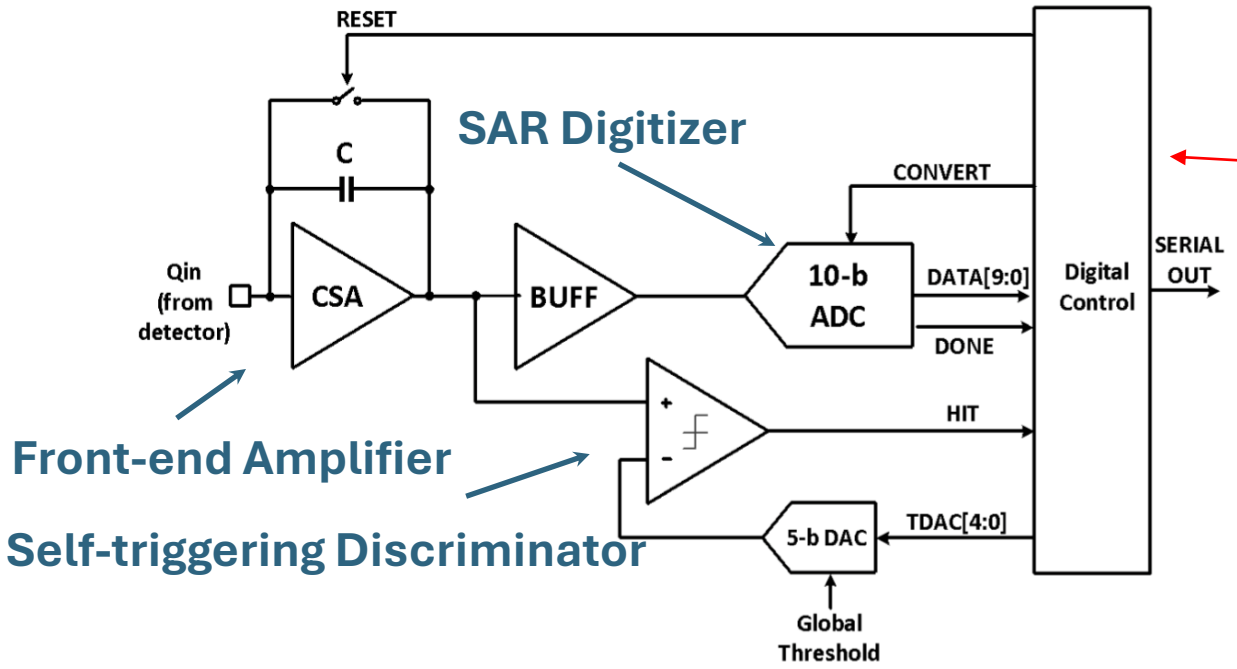

64-channel SoC, in 130nm

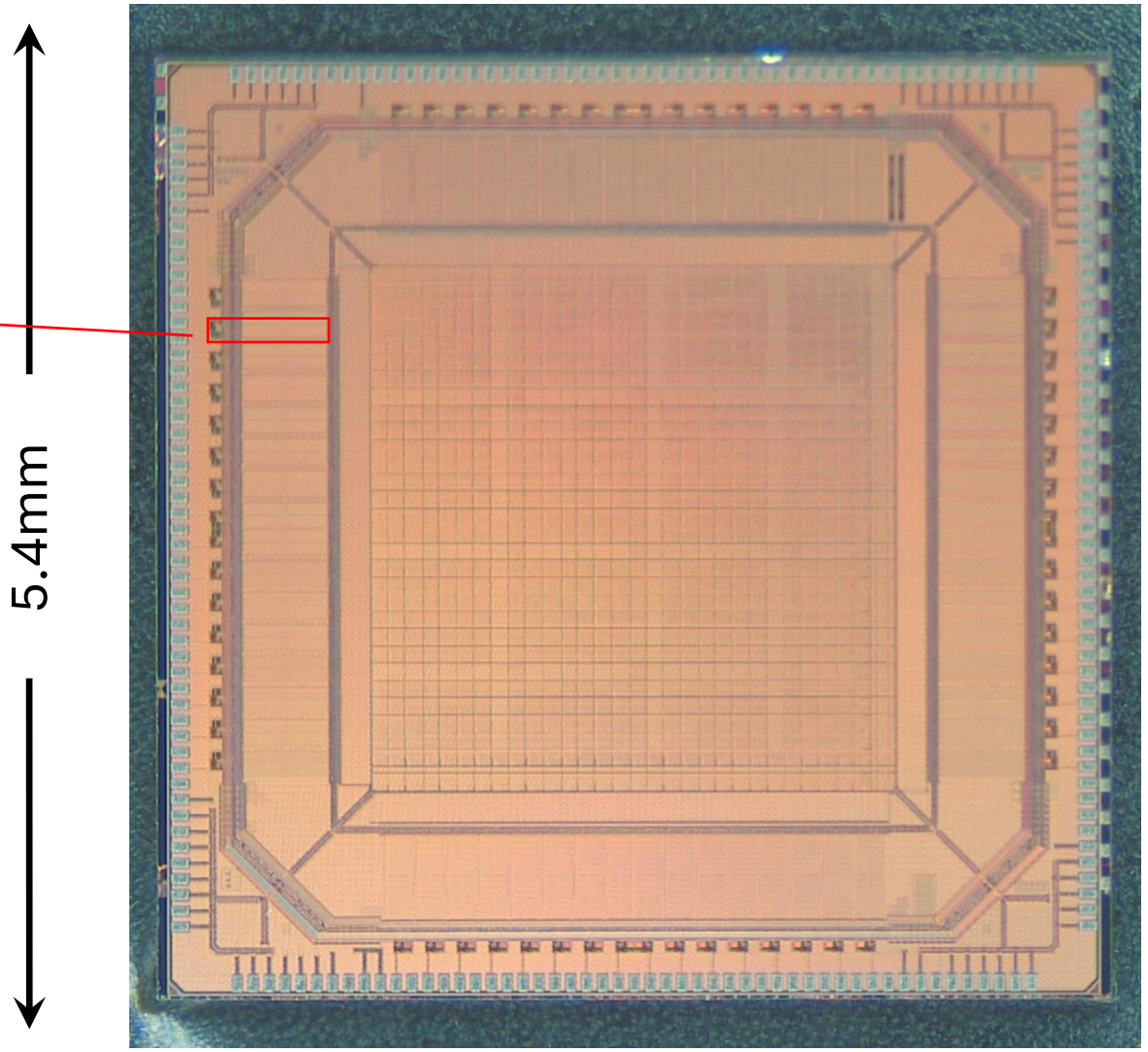

Charge sensing: per-pixel integrating amplifier with self-triggered digitization and readout

Performance

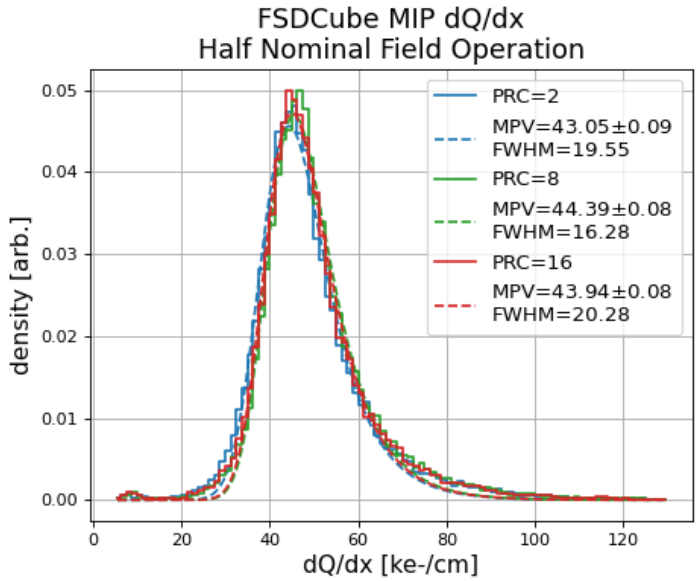

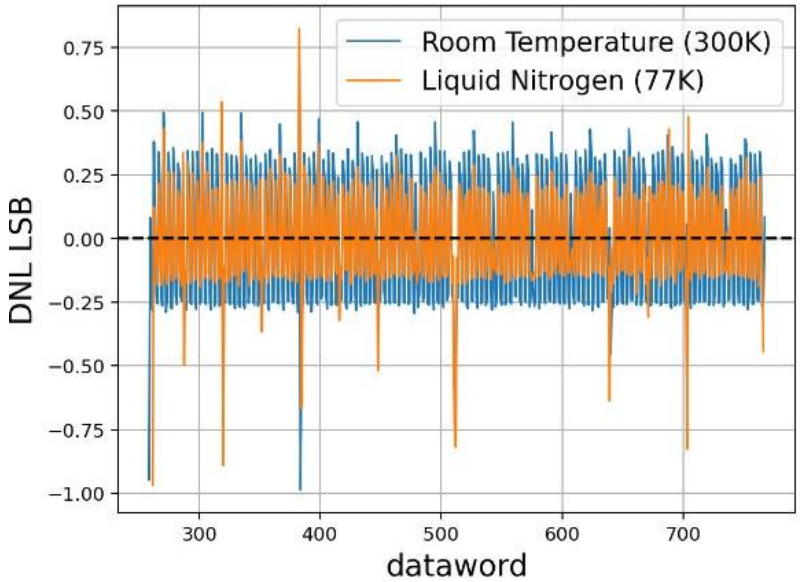

DNL <1 LSB

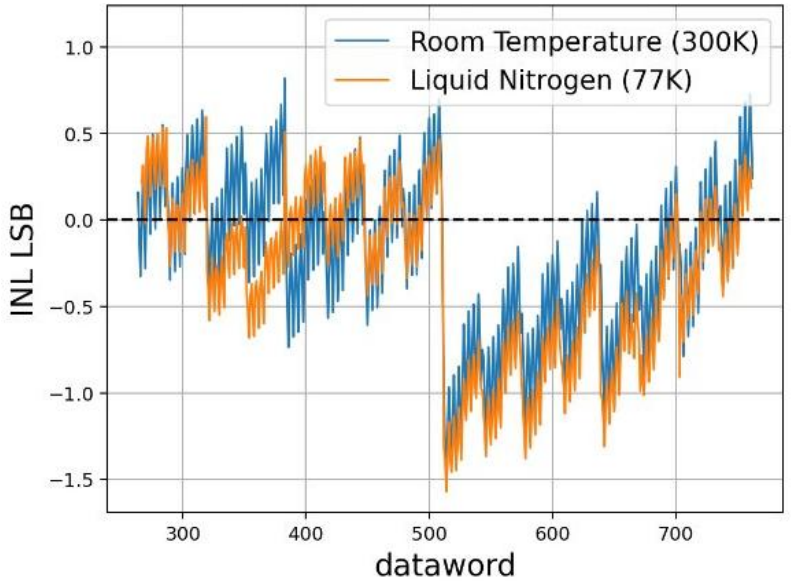

INL <1.6 LSB
(512 is a missing code attributed to a layout artifact)

LArPix-v3a ASIC

- Super source follower front-end buffer
- Asynchronous 10-bit SAR ADC
  - Differential design with bi-directional switching, reduces area and power
  - Asynchronous logic: internally-generated clock speeds ADC conversion

Triggering Schemes

- Self-trigger reset (nominal operating mode): digitize and drain charge after threshold crossed
- Cross-trigger reset: digitize and drain sub-threshold charge based on self-trigger of another pixel
- External-trigger reset: digitize and drain sub-threshold charge based on external signal
- Periodic-trigger reset: periodically digitize and drain sub-threshold charge at fixed cadence on a channel rolling or chip-synchronous basis
- Optional burst modes
    - Fixed burst: process N hit cycles for each self-trigger
    - ADC threshold: continue to process hit cycle until an ADC dataword ceiling (or floor) is exceeded
    - ADC settle: continue to process hit cycles until change in ADC value is below set value

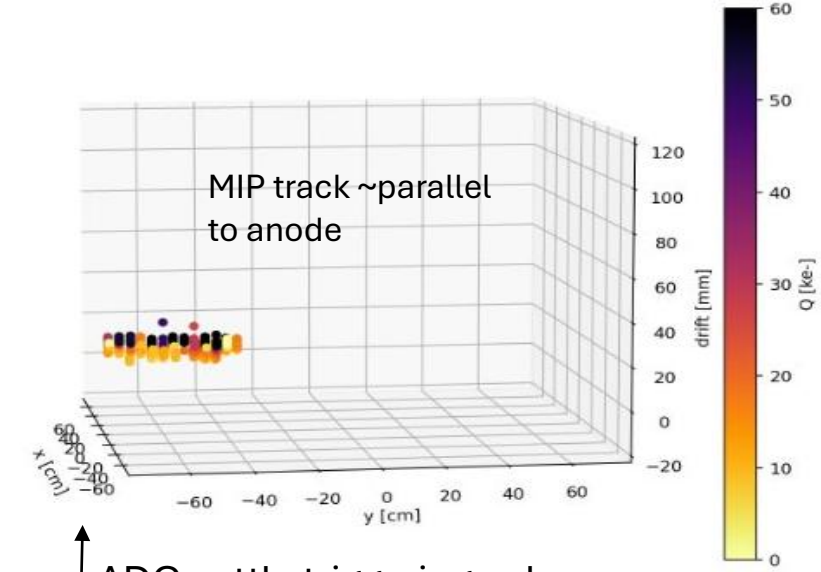

ADC settle triggering scheme

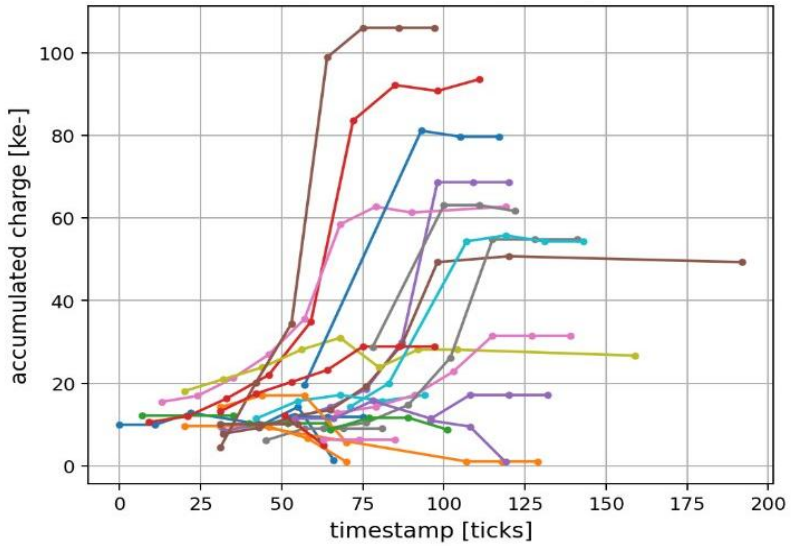

Reset Schemes

- Front-end periodic reset at a configurable cadence on a channel rolling or chip-synchronous basis
  - Highly effective in mitigating detector environment noise
    - Microphonics
    - Cryocooler power cycling
  - Long-range induction mitigation
- 100 ns AFE deadtime incurred with each reset

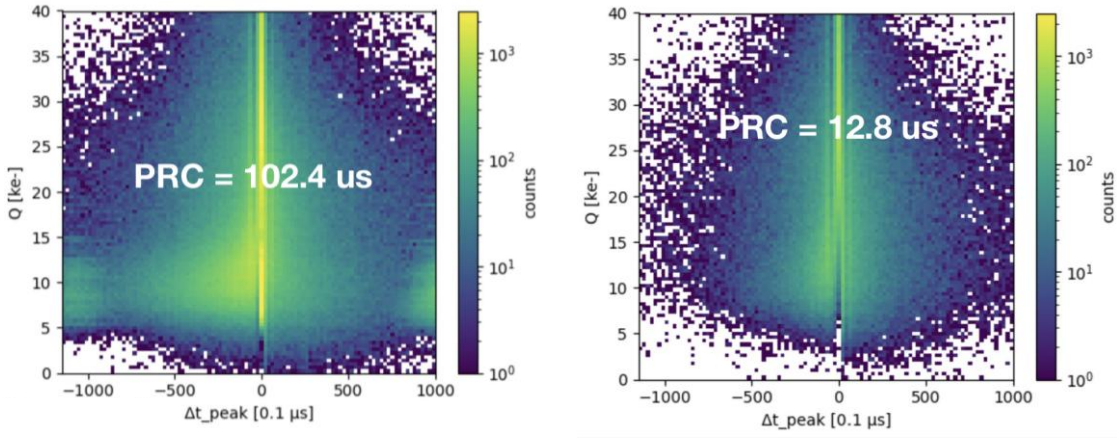

Pixel pedestal RMS (50k channels)

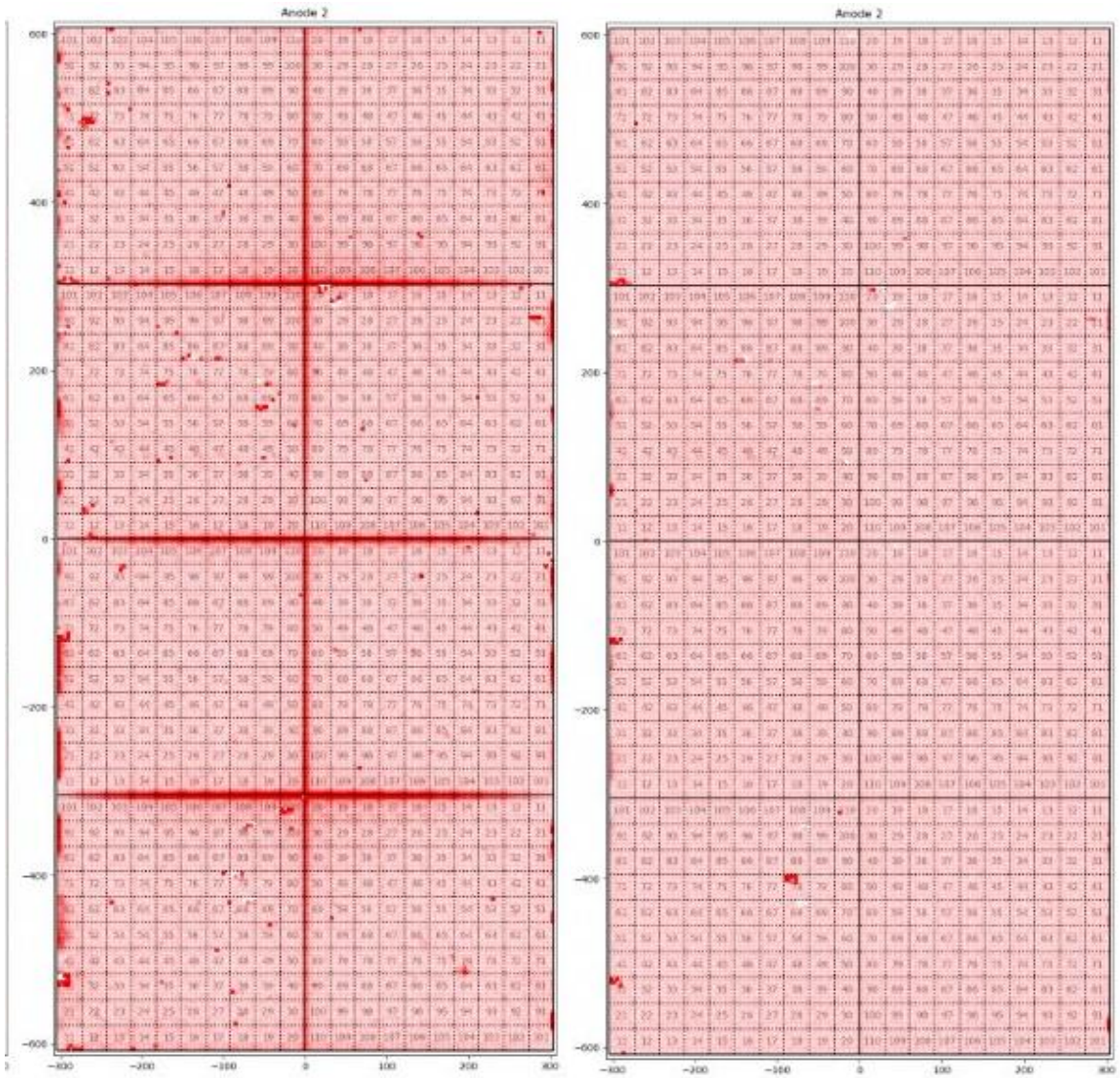

Reset at 2.4 Hz

Reset at 2.4 kHz

LArPix Digital Back-End

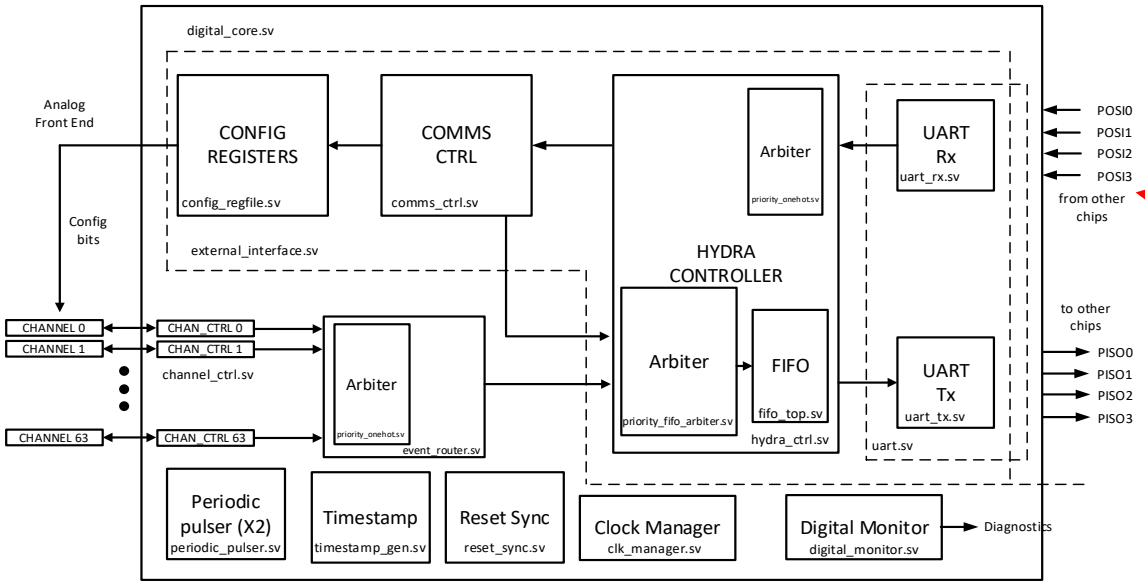

Digital control: data aggregation, amplifier configuration, inter-chip communication

Data transmitted on every rising clock edge (10 Mbit at 10 MHz CLK)

64-channel SoC, in 130nm

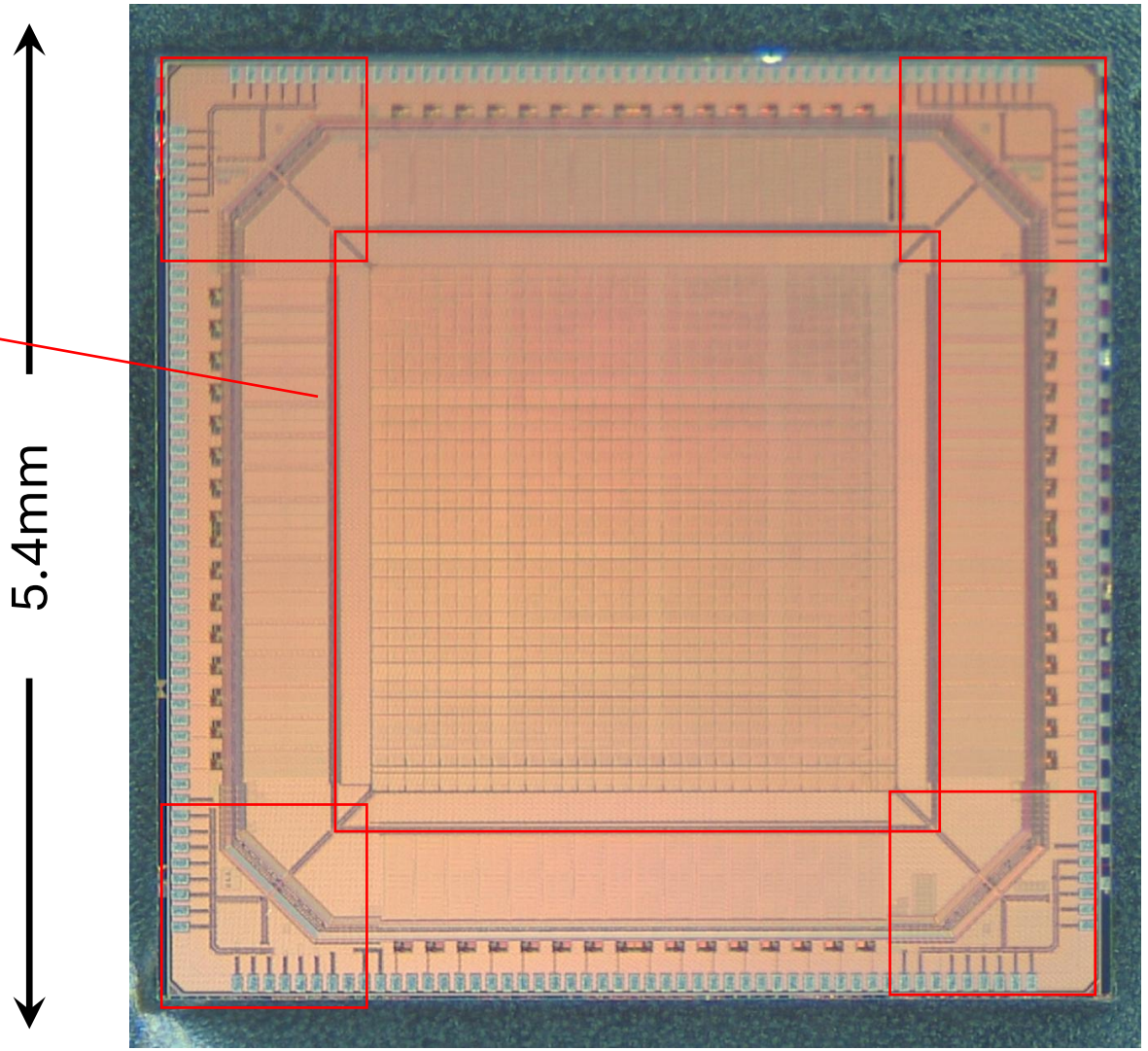

Digital I/O

Custom tunable low-voltage digital transmitter and receiver

- Similar to LVDS in concept, but much lower power: O(10 µW) per transmitter & receiver
- Highly-tunable loop current and termination resistance supports multiple modes of operation (chip-to-chip, chip-to-controller)
- Optional mode for automatic transmitter power-down when no data

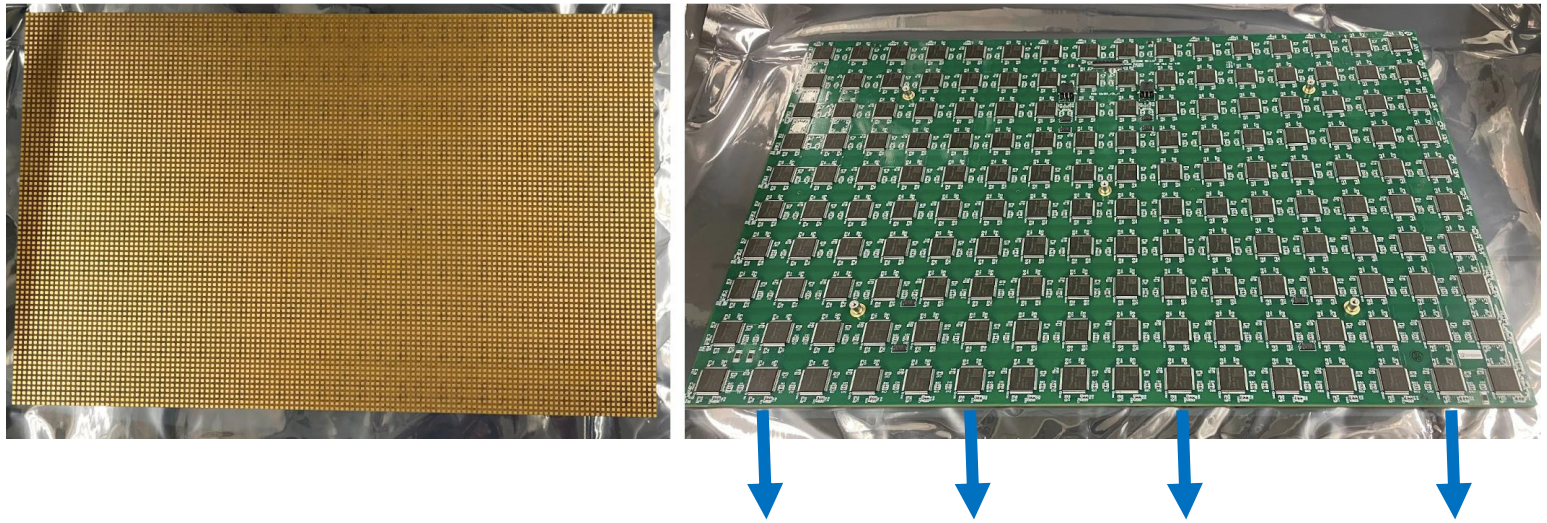

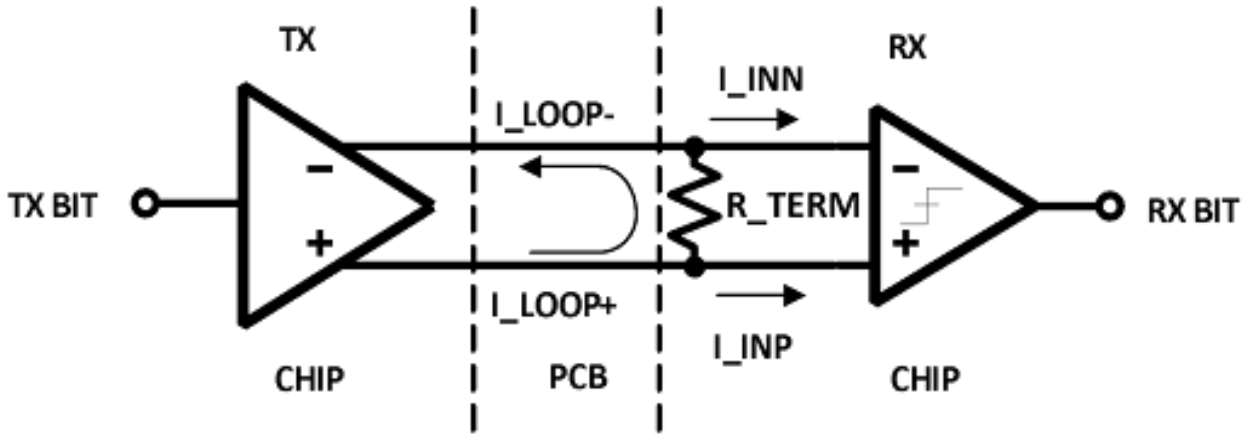

Hydra I/O

- Each ASIC capable of configurable I/O in any cardinal direction
- I/O can occur between any neighboring chips on pixel tile
- ASIC network constructed by explicit configurable connection between neighboring ASICs in a determined fashion

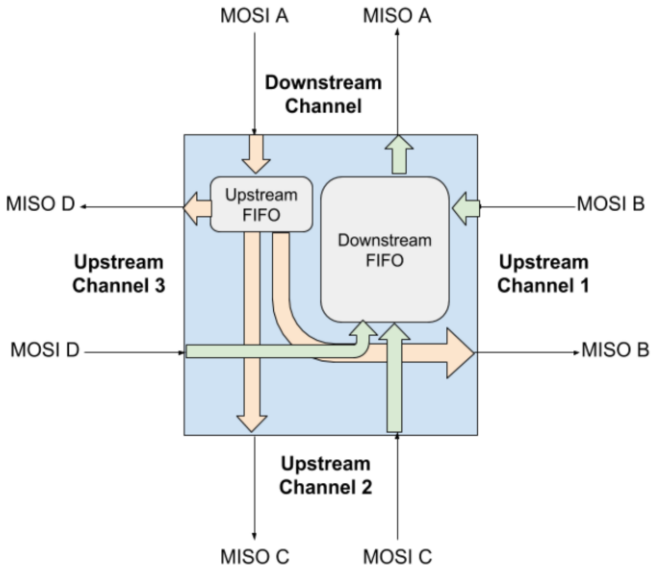

Example 5x5 pixel tile network

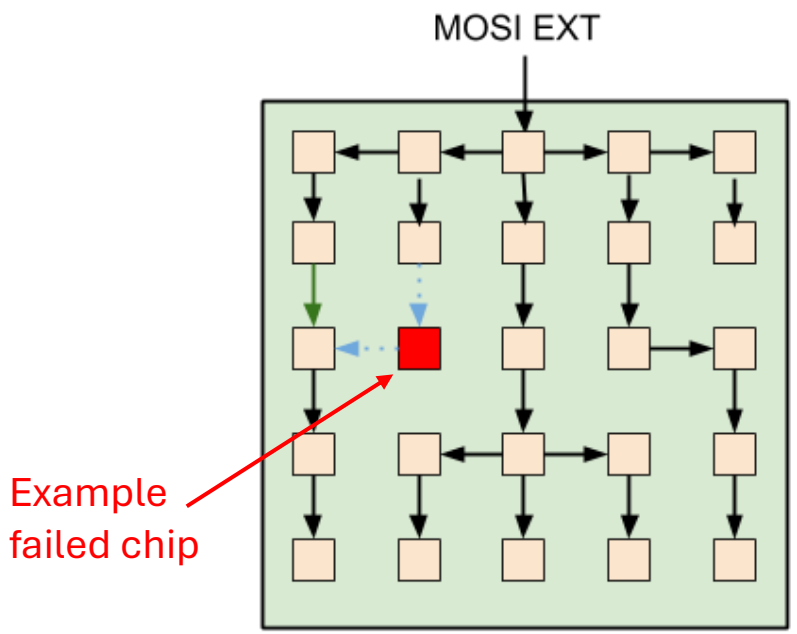

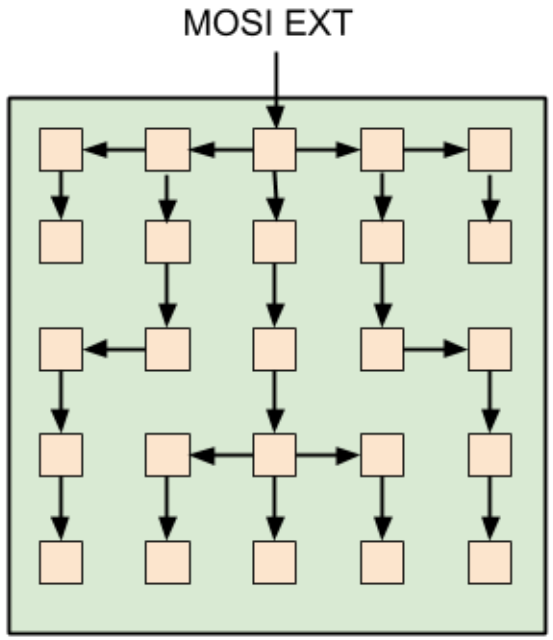

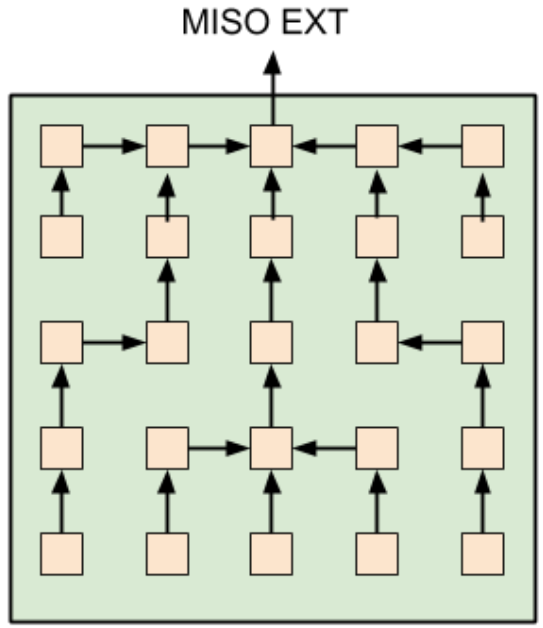

DUNE's First Neutrinos with the 2x2 Demonstrator

Collected 1.5E19 protons on target corresponding to ~30k (anti)neutrino interactions in LArTPC volume

- Eight optically isolated TPCs in 2.4 tonne active mass
- 337k charge-sensitive pixels at ~4 mm pitch operated at 5 kiloelectron pixel threshold
- 29% photocoverage read out by 384 SiPMs

Additional beam anticipated Fall 2026

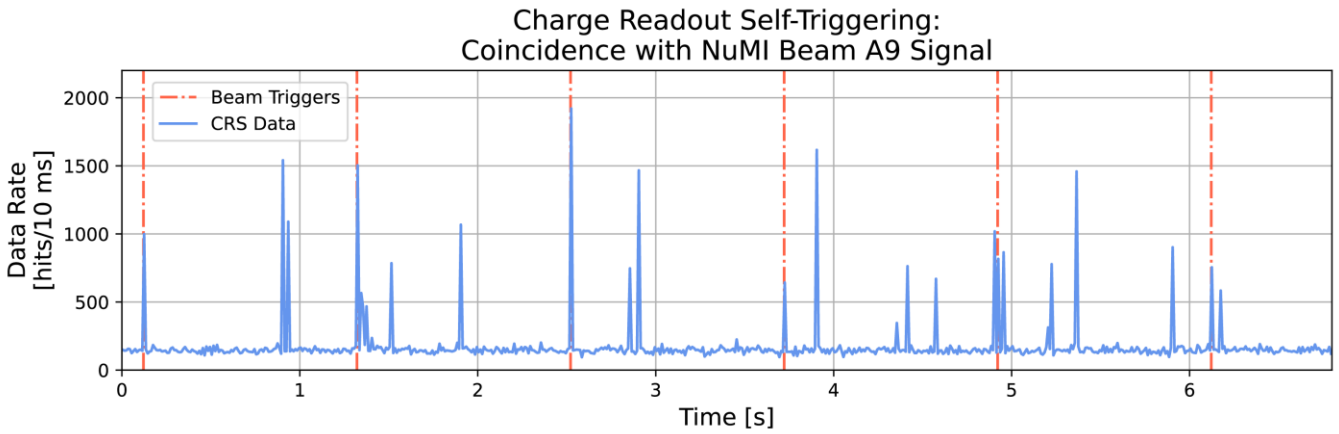

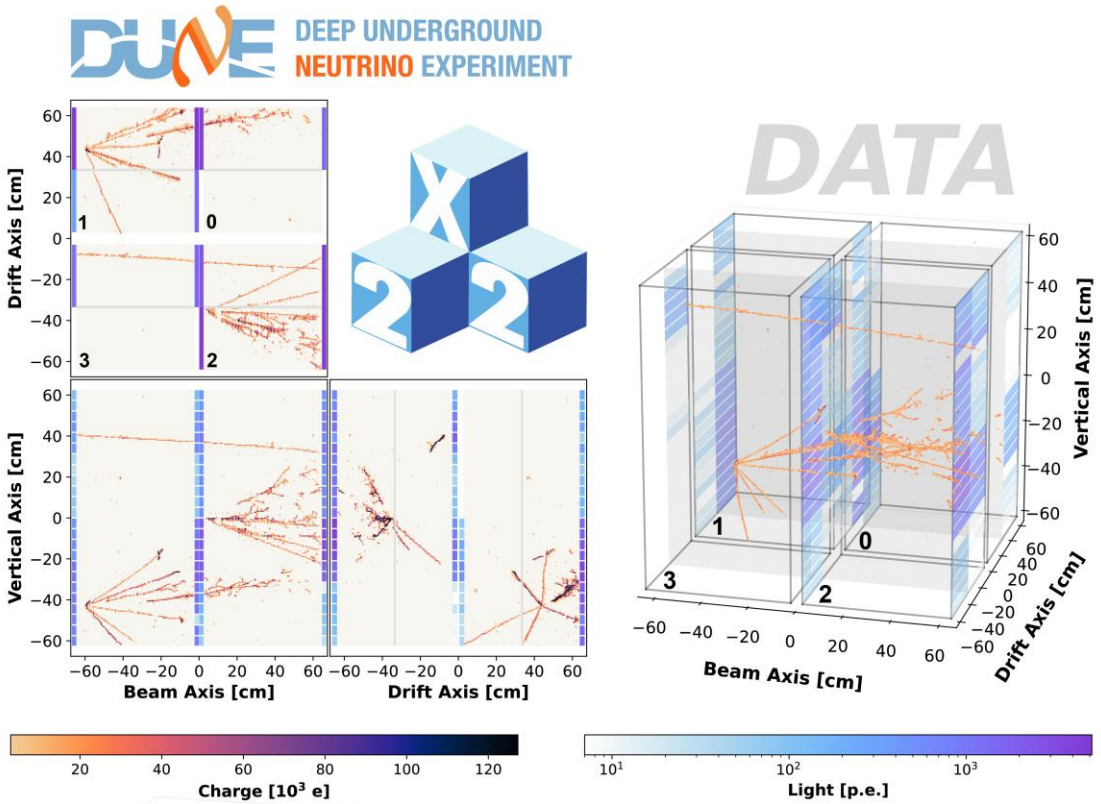

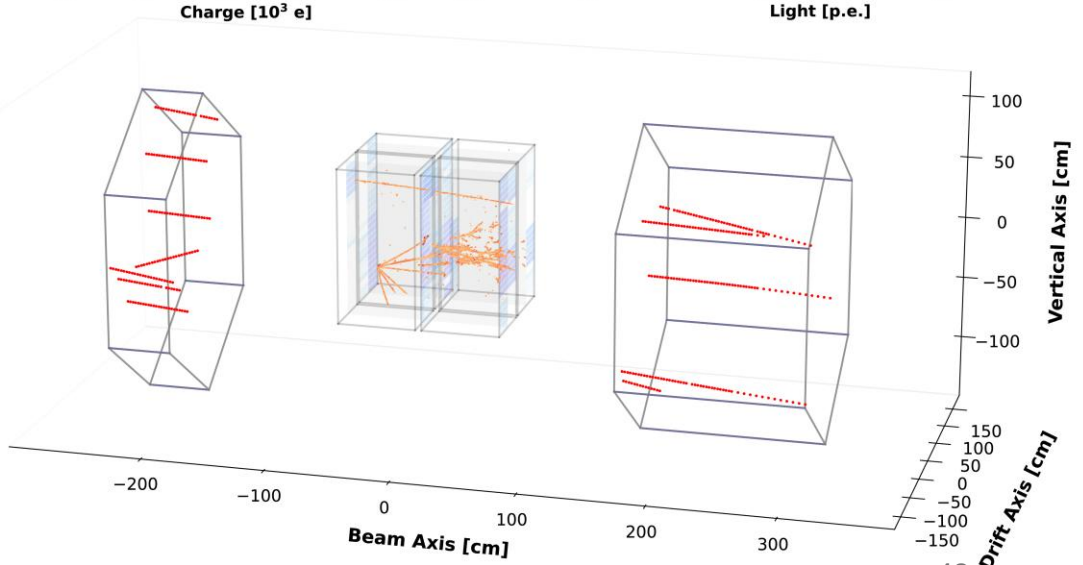

Summary

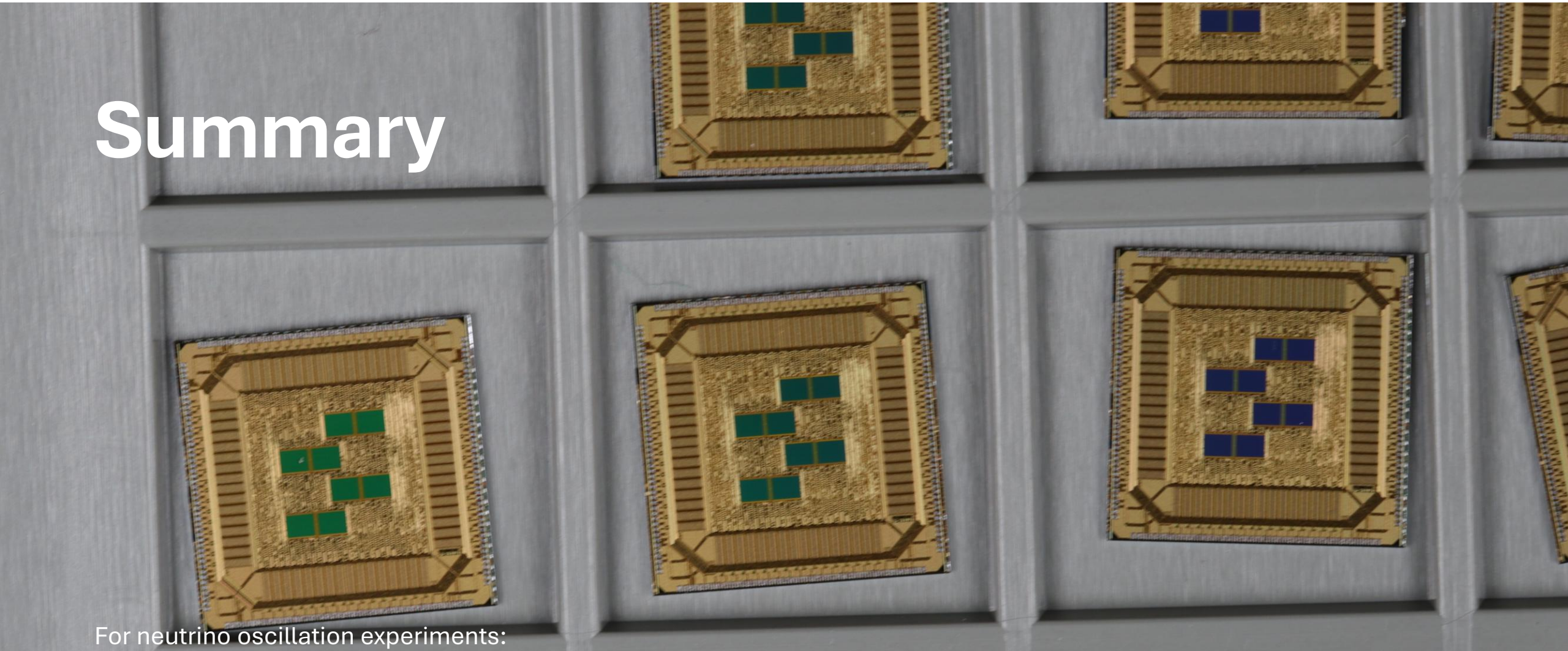

For neutrino oscillation experiments:

- kinematic method ➔ high photocoverage + large mass
- calorimetric method ➔ fine tracking, high scintillation/charge yield + large mass

Final words on the future of detector instrumentation:

- Low background rare event searches ➔ quantum sensing techniques
- High energy physics ➔ microelectronics, especially on-chip AI (significant neutrino-collider synergy)